Elsevier Editorial System(tm) for Journal of Molecular Biology
Manuscript Draft

Manuscript Number: JMB-D-13-00925R1

Title: Relative domain folding and stability of a membrane transport protein

Article Type: Full Length Article

Section/Category: Translation, protein folding, processing and degradation

Keywords: Major facilitator superfamily
Thermodynamics
Single tryptophan residues
Chemical denaturation
Folding free energy

Corresponding Author: Prof. Paula Booth,

Corresponding Author's Institution:

First Author: Nicola Harris

Order of Authors: Nicola Harris; Heather Findlay; John Simms; Xia Liu; Paula Booth

Abstract: There is a limited understanding of the folding of multidomain membrane proteins. Lactose permease (LacY) of Escherichia coli is an archetypal member of the major facilitator superfamily of membrane transport proteins, which contain two domains of six transmembrane helices each. We exploit chemical denaturation to determine the unfolding free energy of LacY and employ Trp residues as site specific thermodynamic probes. Single Trp LacY mutants are created with the individual Trps situated at mirror image positions on the two LacY domains. The changes in Trp fluorescence induced by urea denaturation are used to construct denaturation curves from which unfolding free energies can be determined. The majority of the single Trp tracers report the same stability and an unfolding free energy of ~ +2 kcal.mol-1. There is one exception; the fluorescence of W33 at the cytoplasmic end of helix I on the N domain is unaffected by urea. In contrast, the equivalent position on the first helix, VII, of the C terminal domain exhibits wild type stability, with the single Trp tracer at position 243 on helix VII reporting an unfolding free energy of +2 kcal.mol-1. This indicates that the region of the N domain of LacY at position 33 on helix I has enhanced stability to urea, when compared the corresponding location at the start of the C domain. We also find evidence for a potential network of stabilising interactions across the domain interface, which reduces accessibility to the hydrophilic substrate binding pocket between the two domains.

Relative domain folding and stability of a membrane transport protein

Harris et al.

Response to referees' comments

We thank the referees for their helpful comments and have made changes to the manuscript in accordance with the issues raised by the editor and referees as detailed below. Additionally to improve clarity we have made colour version of the figures.

Editor

We have re-written the abstract and expanded the explanation of the single Trp mutants, p2&5.

It is hard to comment on the absolute magnitude of the free energy value determined for LacY and GalP, in the absence of thermodynamic measurements on other membrane proteins as well as studies using different methods to assess thermodynamic stability in lipid bilayers and kinetic stability. The free energy is small implying that the inherent protein structure has relatively low thermodynamic stability. It could be that the bilayer increases the kinetic stability, or that the absolute magnitude is partly dependent on the renaturing solvent since it is hard to separate the folding systems from the solvent surroundings in membrane protein unfolding studies.

Referee 1

Technical concerns:

1. *DDM CMC in urea*

The CMC of DDM in different concentrations of urea was measured and showed that micelles are present with a DDM concentration of 1mM even at the highest urea concentration of 8M (as previously used for GalP). We have clarified this in the methods (p15) and added a figure S8 to the supplementary information showing the increase in DDM CMC with urea concentration.

2. *Emission wavelength maximum and Cm*

We have also monitored changes in Trp fluorescence intensity, as proposed by the referee, during the urea-induced unfolding. Fluorescence intensity proved to be an unreliable, irreproducible measure. This is due to tendency of LacY to aggregate. Purification of His-tagged LacY on a Ni^{2+} column results in a mixture of primarily monomeric LacY together with dimers (or higher aggregates), with the monomers being purified by a further gel filtration step. The presence of dimers alters the fluorescence spectra and intensity in DDM and urea, but not the shift in the maximum wavelength of the fluorescence band upon urea denaturation. We have added Fig S4 to the supplementary information to show these differences in spectra and a comment to the text (p7).

Although gel filtration was performed on all LacY preparations, dimers or aggregates tend to form at higher urea concentrations during urea denaturation, which alters the fluorescence intensity. Although the changes are small they are not reproducible and introduce errors into the denaturation curves. Thus we use the change in the wavelength of the fluorescence band, which are consistent with the changes in far UV CD. We did not observe any changes in CD spectra for monomer and dimer samples of LacY.

The reviewer acknowledges the inherent problems with far UV CD measurements on membrane unfolding. As a result is not possible to generate high quality denaturation curves from far UV CD data for all single Trp mutants, due to the low signal to noise of the spectra with low protein concentration. Compounding this issue are problems with reproducibility at high urea where the unfolded state is prone to aggregation (as already commented upon in the results p7 first paragraph). Where we have been able to obtain satisfactory data, for $W223_{Phe}$, the Cm values of the fluorescence data is within error of the CD measurement. The denaturation curves determined from the fluorescence data have lower errors than the CD data. It is possible to obtain higher concentrations of WT LacY to improve the CD data quality. A comparison of the C_m values determined for the single Trp mutants from the fluorescence data, as compared to the WT, show that the C_m values of the single Trp mutants may be consistently higher than WT protein. However, the results are within error. Moreover, the difference in magnitudes of the Cm value determined from the fitted data could reflect the different sensitivities of the CD and fluorescence measurements (and the fact that we use fluorescence band wavelength). Whilst this could indicate deviation from a two state model, it does not prove it and we use the simplest model to interpret the results. We have added a table S3 with the C_m values in the supplementary information, together with a comment about them in the text as well as about using a two-state model (p7, p8).

Scientific concerns:

1. *Mutations and denatured state*

It is not possible to conclude that the mutations have altered the secondary structure of the urea-denatured state from the far UV CD spectra. The altered spectral shape primarily arises from the low signal to noise of the data as a result of low concentrations of some of the mutant preparations. We have added a few sentences regarding the possibility that the mutations influence the urea-denatured state, p7.

2. *$W223_{Tyr}$ stability*

We have clarified the comment in the paper; the secondary structure of $W223_{Tyr}$ is more stable to urea denaturation than that of $W223_{Phe}$, as shown by far UV CD spectra (FigS3). It is not possible to

determine an unfolding free energy for $W223_{Tyr}$ because the denaturation curve is altered. We have added a comment to this effect (p9).

3. *E269Q*

A complete investigation of hydrogen bonding, and other interactions, across the domain interface requires substantial further investigation and is beyond the current study. There is a network of interactions at the interface and it is difficult to isolate and delete individual bonds without introducing other interactions. E269 is also directly involved in LacY function and it proved necessary to mutate it to an amino acid of similar size (Q). We have commented on this in the results, p10.

Typos

We have corrected the typos. Note that for Fig3 the graph is labelled as W33 since it shows data for both $W33_{Phe}$ and $W33_{Tyr}$.

Referee 2

General opening comments

The referee is correct in their understanding of the study – that we mutated all native Trps to Phe, or all Trps to Tyr and then in these two background re-introduced single Trps. In line with this referee's comments as well as those of the editor, we have clarified this in the paper and expanded our description of the mutants, p5.

The unfolded state is partly structured, as is typical for unfolding studies on helical membrane proteins. We have stated this in the paper, p6.

Other points:

1. We have moved the main data table from the supplementary information to the main text as table 1.

2. Fig 3B. The data on the RHS are determined from the individual data points from the denaturation curve on the LHS. We have clarified in the paper, p8.

3. *Comment relating to most single Trps show same free energy of unfolding except W33; local versus global stability and relationship to helix insertion mechanism in vivo*

We note that referee 1 concurs with our interpretation of local and global stability, stating "One particularly interesting discovery of this study is the local stability of a few parts of LacY can be different domain (noticeably around W33 and F243) from the global unfolding and the local stability at the pseudo-symmetric positions in each domain is different."

The changes in single Trp fluorescence report on the change in the local environment of each Trp residue, not on the global change in the protein. This is the starting point for interpreting the data. It can be inferred from the single Trp results that the protein unfolds cooperatively from the data, but this is an interpretation of the local measurements. The fact that single Trps at different sites across the protein report similar unfolding free energies does not, however, prove co-operative unfolding.. We have included a short discussion on this, p10-11.

The maximum of the fluorescence band of each single Trp in the folded state differs because the Trps are in different environments. The fluorescence bands shift to similar, but differing extents upon urea denaturation, again showing their sensitivities to their immediate environs. We have added table S2 showing these wavelength values. However, these individual Trps report similar unfolding transitions, which translate to similar thermodynamic stability at that locale. These are thus local stability measurements. We have altered wording at various points in the manuscript to clarify the thermodynamic and local measurements.

W33 is the exception with urea inducing no alterations in Trp fluorescence and thus structural interactions in the vicinity. This does imply, as the referee comments, that there is no change in the structure in this region and that it therefore remains structured in the urea-denatured state. This is what we mean by stable – this structure in this position in the protein on the N domain is more stable to urea denaturation than the corresponding position on the C domain; a point also noted by referee 1.

With regard to the comment about specific helices, these are the locations of the Trp residues, however it is the structure and interactions in the vicinity of these locations, eg W33, that is stable to urea rather than the whole of helix I for example. We have clarified this throughout the manuscript, together with more explicit reference to sensitivity or urea denaturation of thermodynamic stability and altered wording throughout (including in table 2) to avoid reference to stability of whole helices where we mean local structure at the site of a particular mutation. Changes are marked throughout the text.

Our results provide thermodynamic measures of LacY and thus the intrinsic stability of the whole protein as well as that reported at specific locations on the protein. These intrinsic stabilities are likely to relate to those in the cell – particularly with regard to the relative thermodynamic values determined at different sites. Thus, we can speculate that the intrinsic thermodynmiac stabilities in vitro relate to the stabilities in vivo. We have clarified this in the text, with respect to the discussion of helices 1, VII and neighbouring interactions during topology studies in vivo p12.

4. *m values and change in helicity*

The changes in helicity are not particularly small, being around 30% in high urea. The m values may be small when considering water-soluble proteins, but the common interpretation that these m values directly reflect accessibility of urea to the protein structure is different when there is also a micelle solvating parts of the LacY structure. Our results are reproducible and meaningful. The study shows a number of things. Firstly, that LacY is partly susceptible to urea denaturation and shows a similar sensitivity and stability to urea as GalP, thus indicating that the inherent stability measurements are common to more than one protein of the MFS family. We find that a key aspect of urea denaturation is accessibility to the domain interface and substrate binding packet. Furthermore, the study shows that an equilibrium folding study is possible for large hydrophobic, two-domain proteins and the thermodynamic stability of the protein can be determined. The work also starts to identify which regions of the protein are more stable to urea denaturation than others. Moreover it highlights that as pointed out by reviewer 1, that local stability of certain regions of the LacY structure differ and these are not symmetric with respect to domain position.

*Graphical Abstract (for review)

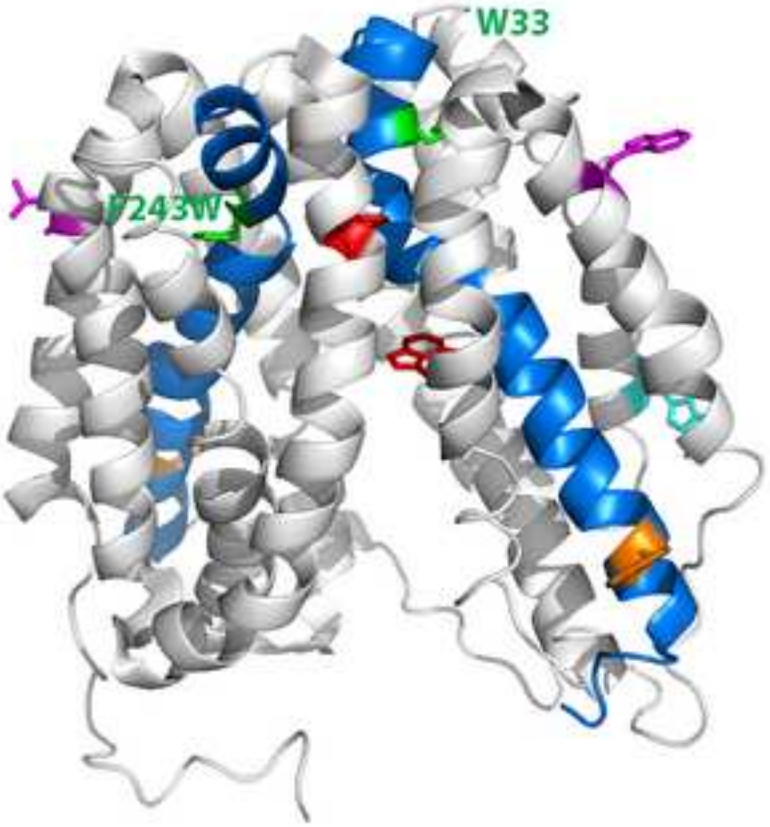

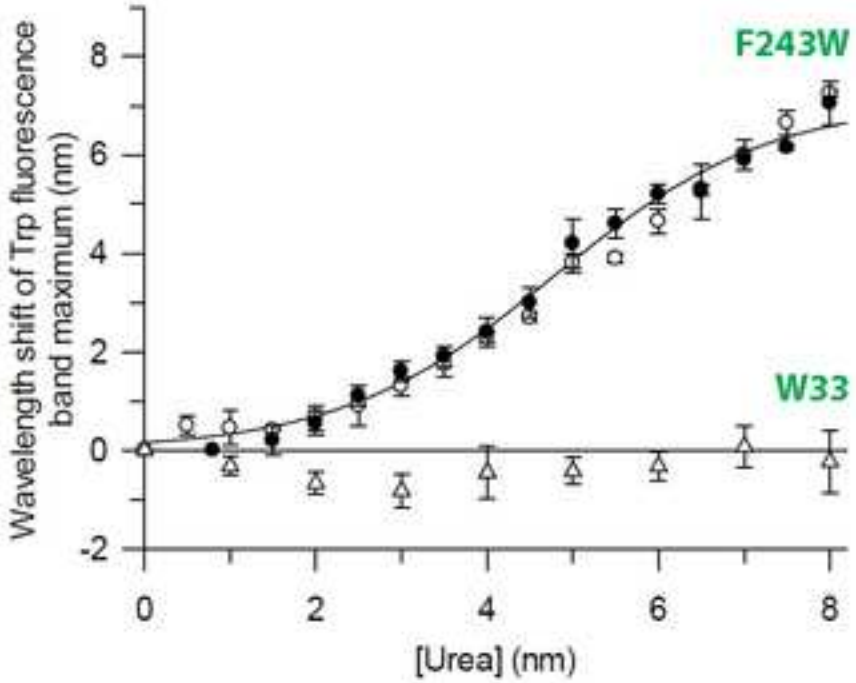

*Research Highlights

Harris et al

Highlights

We introduce a method to determine fundamental folding parameters of an important superfamily of multi-domain membrane transport proteins.

Single tryptophan residues at mirror image positions on the two domains of the membrane transporter show that the first helix of the N domain has enhanced stability

This highlights an unusually stable region on one protein domain that is likely to be significant during cellular folding.

Relative domain folding and stability of a membrane transport protein

Nicola J Harris, Heather E Findlay, John Simms, Xia Liu and Paula J Booth

School of Biochemistry, University of Bristol, Bristol BS8 1TD UK

Correspondence:

Paula J Booth

School of Biochemistry, School of Medical Sciences, University of Bristol, University Walk, Bristol BS8 1TD UK

Tel: +00 44 (0)117 33 12138, Fax: +00 44 (0)117 33 12168, Email: paula.booth@bristol.ac.uk

Abstract

There is a limited understanding of the folding of multidomain membrane proteins. Lactose permease (LacY) of *Escherichia coli* is an archetypal member of the major facilitator superfamily of membrane transport proteins, which contain two domains of six transmembrane helices each. We exploit chemical denaturation to determine the unfolding free energy of LacY and employ Trp residues as site specific thermodynamic probes. Single Trp LacY mutants are created with the individual Trps situated at mirror image positions on the two LacY domains. The changes in Trp fluorescence induced by urea denaturation are used to construct denaturation curves from which unfolding free energies can be determined. The majority of the single Trp tracers report the same stability and an unfolding free energy of ~ +2 kcal.mol^{-1}. There is one exception; the fluorescence of W33 at the cytoplasmic end of helix I on the N domain is unaffected by urea. In contrast, the equivalent position on the first helix, VII, of the C terminal domain exhibits wild type stability, with the single Trp tracer at position 243 on helix VII reporting an unfolding free energy of +2 kcal.mol^{-1}. This indicates that the region of the N domain of LacY at position 33 on helix I has enhanced stability to urea, when compared the corresponding location at the start of the C domain. We also find evidence for a potential network of stabilising interactions across the domain interface, which reduces accessibility to the hydrophilic substrate binding pocket between the two domains.

Keywords

Major facilitator superfamily; thermodynamics; single tryptophan residues; chemical denaturation; folding free energy

Abbreviations

CD, Circular Dichroism; DDM, *n*- dodecyl β-D- maltoside; DOPE, L-α-1,2-dioleoylphospatidylethanolamine; DOPC, L-α-1,2-dioleoylphospatidylcholine; ITC, Isothermal titration calorimetry; GalP, *Escherichia coli* galactose transporter; LacY, Lactose Permease; MFS, Major Facilitator Superfamily; NPG*, p*-nitrophenyl-α-D-galactopyransoside PE, phosphatidylethanolamine; PG, phosphatidylglycerol; SDS, Sodium Dodecyl Sulphate, WT, wild type.

Introduction

Integral membrane proteins adopt diverse structures with differing stability and flexibility as well as numbers of domains or subunits. How much of their protein structure is dictated by the amino acid sequence and how much by the surrounding membrane, additional proteins or other biological factors is largely unknown. Nonetheless, data is accruing on membrane protein folding, ranging from *in vitro* stability and mechanism to co-translational insertion of transmembrane helices and the influence of the surrounding lipids [1; 2; 3; 4; 5]. Sophisticated thermodynamic, kinetic, and structural detail can at present only be derived from *in vitro* study in artificial conditions such as detergents or simplified membranes. Quantitative data on the intrinsic thermodynamic stability of membrane proteins *in vitro* has engendered considerable interest but has only been determined in a few cases [6; 7; 8; 9; 10; 11]. Equally there are few studies of multi-domain protein folding [9; 10], and important questions relating to the stability and cooperativity of the domains are yet to be addressed. Here, we investigate the folding *in vitro* of a flexible, two-domain transport protein, continuing our studies of the most widespread membrane transporter families, the Major Facilitator Superfamily (MFS). This family comprises approximately 25 % of prokaryotic transport proteins and is also prevalent in eukaryotes, notably as sugar transporters [12].

Protein structure within the bilayer falls into two general types: β-barrels and α-helical bundles. We focus on the considerably more abundant latter class of helical proteins that reside in plasma membranes and bacterial inner membranes, where they perform a wide variety of roles as receptors and transporters as well as being directly involved in photosynthesis and ATP production. The nature of their protein scaffold of inherently stable, hydrophobic helices makes them challenging to study. Reversible unfolding has only been demonstrated for a few α-helical membrane proteins [6; 7; 8; 9], but it has proved possible to establish a thermodynamic equilibrium *in vitro* for an MFS protein and determine the free energy for the final folding step, when native ligand binding is recovered [10].

The majority of MFS transporters have 12 transmembrane helices arranged in 2 domains with a substrate binding site located at the domain interface. The binding site seems to be accessible alternately to either side of the membrane, with an apo-intermediate conformation containing an occluded cavity proposed for LacY [13; 14]. The structure of several MFS proteins have been solved to high resolution [15; 16; 17; 18; 19; 20; 21; 22], including the lactose transporter LacY. WT LacY is highly dynamic as shown by the 85-90 % of backbone amide hydrogens exchanging with solvent in < 5 mins in a 3:1 ratio of phospatidylethanolamine (PE) to phosphatidylglycerol (PG) [23]. Crystal structures have been resolved for WT LacY as well as a stable C154G mutant, which binds but does not transport substrate [24]. Both structures are for a conformation with the binding pocket open to the cytoplasm, whilst there are examples of outward open and occluded states amongst the other MFS structures.

Mechanistic folding studies of α helical membrane proteins have been dominated by investigations *in vitro* on the stable, single domain bacteriorhodopsin protein [6]. Thermodynamic measurements have also been achieved for a few other proteins, including bacterial diacylglycerol kinase [7] and the potassium channel KcsA [8]. Recently, we extended the approach to the MFS galactose transporter GalP, of *E. coli*. GalP was reversibly unfolded in DDM micelles by urea, enabling the unfolding free energy to be determined [10]. Moreover, as shown previously for membrane proteins [25; 26], a linear free energy relationship was observed with urea concentration which allows extrapolation to an unfolding free energy, ΔG_u^{H2O} of +2.5 kcal.mol^{-1} in the absence of urea. This provides a reference intrinsic stability measure to quantify stability at specified sites via the change induced in this free energy; $\Delta\Delta G_u^{H2O}$, by a site-directed mutation. GalP loses about a third of its helical structure in 8 M urea, which we suggested was most likely due to urea denaturing helical structure that extends beyond the membrane as well as via the hydrophilic substrate binding pocket between the two domains. Unfortunately the structure of GalP has yet to be solved, hence we translate the approach to the extremely well studied lactose transporter of *Escherichia coli*, LacY, for which results can be interpreted in the context of a known high resolution structure. We exploit the ΔG_u^{H2O} measurement to probe the relative stability at specific sites of the two transporter domains as well as at the domain interface. We combine free energy measurements with site-specific mutagenesis and use single Trp reporters of local thermodynamic stability. LacY has been extensively mutated with only 6 residues in the protein being absolutely required for function, none of which are a Trp [27]. LacY contains 6 native Trp residues, and single Trp mutants of LacY have previously been prepared where the remaining 5 native Trps have been mutated either all to Phe or all to Tyr [28; 29]. Transport activities of these single Trp mutants are 75-100 % of WT LacY, regardless of whether Phe or Tyr is used as the Trp replacement [29]. Replacing native Trps with Tyr resulted in higher overexpression.

Our strategy is to use unique Trp residues to probe particular regions of the protein. This approach assesses the local structural and solvent environment of each Trp, building up a picture of stability across the two domains. For these experiments, we created two series of single Trp mutants. Firstly, the 6 native Trp residues of LacY were all mutated to Phe to give a Trp-less LacY mutant with a Phe background. Additionally, all native Trps were mutated to Tyr, giving Trp-less, Tyr background LacY. Into these Trp-less backgrounds a single Trp was introduced at a specified site. The sites chosen are shown in Fig 1. Firstly we used the locations of the 6 native Trps (positions 10, 33, 78, 151, 171 and 223) and re-introduced individual native Trps into the Phe and Tyr backgrounds. This generated two versions of the same single Trp mutant: one in a Phe background (where all other native Trps are mutated to Phe) and one in a Tyr background (where all other native Trps are mutated to Tyr). We denote the backgrounds with a subscript; thus $W33_{Phe}$ and $W33_{Tyr}$ refer to the single Trp W33 in a Phe or Tyr background respectively, with a Trp at position 33 in the protein. Each of the native LacY Trps is in a different environment (see Fig 1), either buried within the helical bundle, in the hydrophilic binding pocket or surface exposed to lipids. Thus the native Trp positions

report on a number of different locations across the protein. However, the native Trps are primarily located in the N domain of LacY, with only one in the C domain. We therefore created additional single Trp mutations with non-native Trps introduced into the C domain, at positions that mirrored those of the native N domain Trps. These non-native single Trp mutants are designated by the mutation, using a subscript to denote the Phe or Tyr background. Again two versions of each non-native single Trp were made; $F261W_{Phe}$ and $F261W_{Tyr}$ thus refer to the single Trp mutant F261W in a Phe or Tyr background respectively, with a Trp at position 261 introduced by mutation of F261. Additionally, we quote in brackets the domain and helix location of the single Trp together with its local environment. Thus position 243 is on helix VII in the C domain at an interhelical position, which we refer to as: $F243W_{Phe}$ (C domain helix VII; interhelix). This array of single Trp mutants allows us to compare intrinsic stability at equivalent structural sites on the two domains of LacY. We use Trp fluorescence to follow changes in the local structure induced by urea denaturation, together with far UV circular dichroism (CD) to monitor the changes in the overall protein secondary structure content. Additionally, we use aqueous fluorescence quenchers of Trp residues in the binding site to correlate binding pocket accessibility with urea stability for stabilising mutations at the domain interface.

Results

Reversible unfolding of LacY

Equilibrium chemical denaturation provides a useful method for free energy determination. LacY in 1 mM dodecylmaltoside (DDM) was reversibly denatured by urea, as previously shown for GalP [10]. Far UV CD showed the same, ~30 %, reduction in WT LacY α helical structure (with all native Trps present) in 8 M urea as for GalP (as estimated from the reduction in the negative band intensity at 222 nm indicative of α helical structure; see Fig 2A). The 8 M-urea denatured state of LacY (and GalP) thus contains ~70 % of the native helical structure. Such structured, chemically-denatured states are usual for transmembrane helical proteins since denaturants such as urea or SDS do not fully unfold transmembrane helices. Upon refolding LacY from 8 M urea, by dilution into DDM detergent micelles, the far UV CD spectrum returned to that of the original purified native protein. Isothermal titration calorimetry (ITC) binding measurements with the lactose analogue, *p*-nitrophenyl-α-D-galactopyransoside (NPG) demonstrate that native binding activity returns once the protein has refolded, with a K_d of 93 µM, compared to the original, folded WT K_d of 10 µM (see Fig S1).

Equilibrium denaturation curves were determined as reported previously for GalP [10], by incubating originally folded LacY (in DDM) in increasing concentrations of urea (see Fig 2B). The refolding curve was generated by first unfolding LacY in 8 M urea, then refolding by dilution into different urea concentrations.

As found previously for GalP, the folding and unfolding curves overlay, which is consistent with a reversible reaction. Assuming the simplest model, the data were fit to a two-state reaction (Fig 2B), which is also in line with the previous report on GalP. Partially unfolded LacY was more prone to aggregation than GalP at high urea concentrations (> 6 M), which affected the CD data quality especially for refolding data for which signal to noise is lower as a result of lower protein concentrations. The higher quality unfolding data were fit to a two-state equation, giving an unfolding free energy in the absence of urea, ΔG_u^{H2O}, of +2.7 ± 0.6 kcal.mol^{-1} at pH 7.4. The free energy of unfolding, ΔG_u was also calculated at different urea concentrations and found to be linear with urea concentration, giving a ΔG_u^{H2O} of +2.5 kcal.mol^{-1} by extrapolation to zero urea (see Fig S2). These ΔG_u^{H2O} values for LacY are very similar to that obtained for GalP, of ΔG_u^{H2O} of + 2.5 kcal.mol^{-1} (at pH 8 [10]).

Single Trps as site-specific reporters of stability

The 6 native Trps of LacY complicate the fluorescence spectra of the wild type protein and changes therein upon unfolding. Thus we employ single Trp mutants. Far UV CD spectra showed that the secondary structure of all the single Trp mutants in a Phe background exhibited similar stability to urea as WT LacY, with an approximately 30 % reduction in secondary structure in 8 M urea (Fig 3A and Fig S3). The apparent spectral shape changes for certain Trp mutants arise from lower signal to noise for the data from mutant LacY proteins for which lower expression and protein concentrations was found. This issue of lower quality spectra is more pronounced for the urea-denatured state as the presence of urea also reduces spectral quality and the characteristic α helical CD signal at 222 nm is smaller. Since the urea-denatured state is partly structured it is possible that the Trp mutations induce alterations in this unfolded state, an issue previously discussed for helical membrane protein unfolding investigations [30]. However, it is not possible to conclude that the urea-denatured states of the mutants have different secondary structure from these CD spectra.

The changes in single Trp fluorescence were monitored during urea-induced unfolding and refolding. Trp fluorescence of all but one single Trp ($W33_{Phe}$) in a Phe background decreased in intensity and shifted to longer wavelengths upon urea denaturation. No change in fluorescence was observed for $W33_{Phe}$ (N terminal helix I, interhelix; Fig 3B (top left) and Table S1). For these unfolding measurements, the red shift in the fluorescence emission band was used as a measure of unfolding. Using the fluorescence intensity to mmoitor unfolding was unreliable and irreproducible due to the formation of dimers and aggregates at higher urea concentrations (Fig S4). The increase in the wavelength of the emission band maximum with increasing urea concentration is indicative of increased Trp exposure to hydrophilic or polar solvents and therefore monitors unfolding. The wavelength of the fluorescence band maxima for each single Trp mutant differ in the folded and urea states, illustrating their different solvent exposure and environment (see Table S2). Urea-denaturation curves were generated from the change in the wavelength of the fluorescence band

maxima against urea concentration (Fig 3B, Fig S5). Upon refolding, the original fluorescence wavelength was recovered for each single Trp and the refolding curves overlaid the unfolding curves, showing reversible unfolding as indicated by CD for WT LacY (Fig 2B). This enabled ΔG_U^{H2O} values to be determined from the fluorescence denaturation curves. The fluorescence-derived curves could be fit with a two state, equilibrium reaction. ΔG_U^{H2O} values were obtained either from the fit to the denaturation curve, or by evaluating the equilibrium constant for the assumed two-state reaction, and thus ΔG_U, at different urea concentrations and extrapolating to zero urea, as described previously [6; 10]. Fig 3B shows the latter linear free energy plots for $F243W_{Phe}$ and $W223_{Phe}$ (both on C domain helix VII). ΔG_U^{H2O} values were determined for the Phe background single Trp mutants and found to be similar to the WT LacY ΔG_U^{H2O} of +2.5 kcal.mol^{-1} determined from CD data (see Table 1). For example, ΔG_U^{H2O} for $F243W_{Phe}$ and $W223_{Phe}$ were +2.2 kcal.mol^{-1}. From these two-state fits an unfolding transition midpoint, Cm, is also derived, for which the values are also found to be similar for both WT and the single Trp mutants (Table S3). The gradient, m_U^{H2O}, characterising the linear dependence of ΔG_U on urea (for example as shown in Fig3B) was also found to be similar for the Trp mutants (Table S3). This analysis of the single Trp fluorescence data gives a local thermodynamic measure of stability because it is determined from a site-specific reporter.

Table 2 summarises results of single Trp pairs that exhibited differing behaviour, giving insight into relative domain stability and resistance to urea denaturation. The only pair of Trp mutants to exhibit differing degrees of unfolding in chemical denaturants, when measured by intrinsic Trp fluorescence, is that on the first helix of each domain. The Trp fluorescence of $W33_{Phe}$, on helix I of the N domain is unchanged by urea indicating resistance of the local protein structure to urea denaturation. In contrast, the equivalent C domain single Trp $F243W_{Phe}$ on helix VII exhibits the same urea-induced fluorescence changes and thus local unfolding as the other single Trp mutants studied (Fig 3B and Table 2). W33 is a native Trp, but F243W is a new Trp introduced at position 243 on the C domain through mutation of Phe. The introduction of this non-native Trp in $F243W_{Phe}$ does not however affect the overall protein stability with respect to secondary structure denaturation by urea, which is the same as for both W33 and WT LacY (Fig 3A). Thus, the Trp fluorescence changes of $W33_{Phe}$ and $F243W_{Phe}$ report upon the local Trp environment. The aqueous accessibility of $W33_{Phe}$ and $F243W_{Phe}$ in the folded protein was assessed by exposure to acrylamide quenching of Trp fluorescence. The two Trps had similar Stern-Volmer constants (K_{SV}); K_{sv}, 1.76 ± 0.07 M^{-1} for W33 and 1.48 ± 0.12 M^{-1} for F243W (Fig S6). $W33_{Phe}$ and $F243W_{Phe}$ therefore have similar accessibility to urea in the folded state and exhibit similar overall secondary structural loss in urea, but have different Trp fluorescence changes.

Stable, single Trp mutants in a Tyr background

The single Trp mutants were also made with a Tyr, as opposed to Phe, background. All but one single Trp mutant with a Tyr background showed an increased stability to urea denaturation over both WT and the

Phe background counterparts, with little or no reduction in secondary structure in 8 M urea (Fig S3). W151 (N domain, helix V, domain interface) was the only single Trp mutant to show a similar, WT, reduction in secondary structure in both a Phe and Tyr background.

$W223_{Tyr}$ is at the cytoplasmic end of the first helix of the C domain, helix VII. The secondary structure of this Tyr background mutant, $W223_{Tyr}$, was more stable to urea denaturation than the Phe background equivalent, $W223_{Phe}$. The far UV CD spectra of $W223_{Tyr}$ showed a smaller reduction in the intensity of the negative 222 nm band indicative of helical structure (Fig S7). In contrast to all other Tyr background mutants, including its partner $W10_{Tyr}$ on helix I, $W223_{Tyr}$ has a larger red shift in fluorescence than its Phe background equivalent, $W223_{Phe}$ upon urea denaturation. This suggests greater local unfolding in this cytoplasmic region of helix VII (see Table 2 and Fig S7). The fluorescence emission bands of folded and urea-denatured $W223_{Tyr}$ states were also blue shifted to lower wavelengths by 14 nm and 11 nm, respectively, relative to the folded and unfolded state of $W223_{Phe}$ (Fig S7 and table S4). These large blue-shifts suggest that W223 in a Tyr background is in a more non-polar environment, with a decreased aqueous exposure, than W223 in a Phe background. These variations in the fluorescence spectra of $W223_{Tyr}$ and $W223_{Phe}$ suggest slightly different behaviour of the Tyr background mutant $W223_{Tyr}$ to the other single Trps reported here, with local changes in the vicinity of position 223 on helix I being different in a Tyr as compared to a Phe background. The fluorescence denaturation curve of $W223_{Tyr}$ is also different in that it does not plateau at high urea concentrations. Thus it is not possible to fit a two-state reaction and determine the ΔG_U^{H2O} for $W223_{Tyr}$.

Domain interface

All single Trp mutants were more stable to urea denaturation in a Tyr than in a Phe background, except $W151_{Tyr}$ on the N domain at the domain interface. $W151_{Tyr}$ contains a Trp at position 151 in the domain interface, with all other native Trps mutated to Tyr. In all the other single Trp, Tyr background mutants W151 is mutated to Tyr. We therefore investigated whether a single Trp to Tyr mutation at this position, W151Y, could be responsible for the increased Tyr background stability. The mutant W151Y has only the Trp at position 151 substituted by Tyr with the other five native Trps being present. W151Y was found to be more stable with respect to urea denaturation of secondary structure than both WT and $W151_{Tyr}$, which is consistent with the single Trp to Tyr change at 151 being primarily responsible for the increased stability of the Tyr background mutants. W151Y was resistant to urea denaturation, with no reduction in secondary structure (Fig 4A) in line with the Tyr background mutations. W151 lies at the domain interface (Fig 1) and the aqueous accessibility of this interface was probed by acrylamide quenching of Trp fluorescence. The aim was to assess aqueous accessibility of a Trp at this interface in a more stable (i.e. Tyr background) and less stable (i.e. Phe background) mutant. Since W151 has the same stability in both a Tyr and Phe background, quenching of the single Trp mutant F261W was measured. F261W lies at the domain interface

on the C domain, but in a mirror image position to the N domain W151. F261W can be used to illustrate the difference in quenching with stability, since F261W also has increased stability in a Tyr background over a Phe background (Fig S3). The Trp at position 261 showed less quenching in the more stable Tyr background ($F261W_{Tyr}$) than Phe ($F261W_{Phe}$), with K_{SV} values of 0.52 ± 0.06 M^{-1} and 1.67 ± 0.11 M^{-1} respectively, indicating a lower exposure of Trp to acrylamide in the Tyr background (Fig 4B). The K_{SV} value of $F261W_{Phe}$ corresponds well with that previously published for $W151_{Tyr}$ of 2.01 ± 0.1 M^{-1} [31], indicating similar accessibility of $W151_{Tyr}$ to the Phe single Trp mutants.

Additional hydrogen bonds involving the newly introduced Tyr at position 151 were investigated as a possible cause of the increased stability of W151Y. Potential hydrogen bonding partners of W151Y across the domain interface were deleted (Fig 5A); T265, E269 and H322, and the stability of double mutants, which contained one of these deletions combined with W151Y, were measured. If hydrogen bonding is a factor, these deletion mutants should be less stable than W151Y. The potential hydrogen bonding partner mutations were also incorporated into the single Trp $W10_{Tyr}$, to measure them in a Tyr background. Thus for example $W10_{Tyr}$/E269Q lacks a possible E269-W151Y interaction as well as having all native Trps replaced by Tyr, except W10. E269 is important for LacY transport and for these initial investigations of interactions across the domain interface, a conservative mutation with respect to size was made. E269 was mutated to a residue of similar size, Gln, despite the fact that the newly introduced residue could introduce new interactions from the Gln amide group. T265V had no effect on stability, whilst the double mutants W151Y/H322F and W151Y/E269Q were slightly less stable than W151Y (see Fig 5D). $W10_{Tyr}$/E269Q was the only mutant studied to have decreased stability, with a significant reduction in helicity in urea (Fig 5B), although this mutant could not be refolded, and thus showing irreversible denaturation of $W10_{Tyr}$/E269Q. LacY with all Trp mutated to Tyr is also slightly less stable than W151Y, thus the reduction in stability of $W10_{Tyr}$/E269Q compared to W151Y is due both to the additional native Trp-Tyr mutations (i.e. as present in $W10_{Tyr}$), as well as hydrogen bond or other interactions that are affected by E269Q and H322F. E269Q also reduced the stability of C154G; a stabilising mutation in the domain interface.

Discussion

Site-specific reporters across LacY reveal that the two domains exhibit similar thermodynamic stability, apart from in the region of the first helix of each domain. The fluorescence emission of each single Trp depends upon the local solvent environment of the Trp residue in question. Hence, the Trps in different positions on the folded protein exhibit different wavelengths for the positions of their fluorescence band maxima, reflecting their contrasting environments (Table S2). The individual Trps studied here therefore report on local changes in the protein structure and solvent surroundings at the location of the Trp. The separate Trps also exhibit differing shifts in the position of their emission maxima upon urea denaturation,

again showing their sensitivity to changes in the local environment. However, the unfolding transitions these shifts measure (apart from W33) are remarkably similar, revealing comparable unfolding free energies, analogous dependence upon urea and in turn equivalent thermodynamic stability at zero urea. This strongly implies that at each site studied on LacY (apart from position 33) the apparent unfolding free energy is similar. Moreover, these thermodynamic values reported by the change in position of the fluorophore emission bands concur with those determined from changes in CD spectra. The latter reports upon the overall reduction in protein secondary structure upon urea denaturation. Thus the individual thermodynamic stabilities reported by the single Trps at sites across the protein are the same as the global thermodynamic stability of the protein, determined from CD spectra. This suggests cooperative unfolding of LacY. Of the single Trps investigated only one at position 33 of LacY gives different results. Although the same overall reduction in secondary structure as WT occurs upon urea denaturation for $W33_{Phe}$, there is no change in the fluorescence emission band of the Trp. Thus, there is no change in protein structure induced by urea in this region of LacY and therefore the structure of the protein in the vicinity of position 33 on helix I remains structured in the urea-denatured state. The protein structure at this site on the N domain (position 33) is more stable to urea denaturation than the corresponding position on the C domain (position 243). W33 is buried within the helical bundle of the N domain on helix I; hence W33 reports an enhanced local structural stability and resistance to urea denaturation compared to the equivalent position 243 on helix VII in the C domain (see Fig 1). The unfolding free energy reported by $F243W_{Phe}$ is similar to WT and the other single Trp mutants. Additionally, the fluorescence data from the Tyr background mutant $W223_{Tyr}$ suggests local unfolding at the cytoplasmic end of helix VII, in contrast to the corresponding position, $W10_{Tyr}$, on helix I. Thus, the intrinsic stability of the N domain in the region of helix I is greater than that of helix VII, with the structure in the locale of positions 243 and 223 on helix VII being more susceptible to unfolding by urea. Across the rest of the protein individual Trp residue pairs, in a Phe background, at mirror image locations on the N and C domains all report the same unfolding free energy as WT; these include Trps at positions 10, (N, helix I), 78 (N, helix III) and 223 (C, helix VII) all near the cytoplasmic loops on each domain; 151 (N domain, helix V) and 261 (C domain helix VIII) at the domain interface, as well as 171 (N domain helix VI) and 383 (C domain helix XII) facing the detergents or lipids (Fig 1).

Single Trp reporters of local unfolding

The unfolding free energies are determined from urea denaturation curves, with extrapolation to ΔG_u^{H2O} in the absence of urea, as determined previously for the MFS protein, GalP [10]. These are thus intrinsic thermodynamic stability values independent of urea concentration. Denaturation curves obtained from the reduction in secondary structure, as determined by far UV CD, for all single Trp mutations with native Trps mutated to Phe (including $W33_{Phe}$ and $F243W_{Phe}$) are consistent with WT LacY and GalP unfolding free energies of ~ +2 kcal.mol^{-1}. Trp fluorescence-derived curves also give unfolding free energies of ~ +2 kcal.mol^{-1} for all single Trp, Phe background mutants, except $W33_{Phe}$, for which there is no change in W33

fluorescence. Therefore no thermodynamic information can be gained from the fluorescence data with regard to $W33_{Phe,}$ although the results show that the protein structure in the region of position 33 on helix I is resistant to urea denaturation. Both W33 and F243W are equally accessible to aqueous phase fluorescence quenchers in their folded states. Thus the Trp fluorescence band change and unfolding free energy of $F243W_{Phe}$ upon urea denaturation, and lack of for $W33_{Phe}$, report upon the local Trp environment. Whilst far-UV CD derived denaturation, reflecting the overall reduction in secondary structure in urea, is the same for both $W33_{Phe}$ and $F243W_{Phe}$, the single Trp fluorescence denaturation curves from the W33 reporter reveals that this region of the protein is more resistant to urea denaturation than the corresponding region on the C domain, reported by F243W. The Trp fluorescence changes report alterations in both secondary and tertiary structure.

Mutating the native Trps of LacY to Tyr resulted in single Trp mutants that were more stable than WT LacY and the corresponding Phe background mutants, except for $W151_{Tyr}$ at the domain interface, which had similar stability to $W151_{Phe}$ and WT (Fig S3). Additionally, $W223_{Tyr}$ contrasts with the other single Trp, Tyr background mutants in that the fluorescence band suggests $W223_{Tyr}$ is in a more non-polar environment than $W223_{Phe}$. In all other cases studied the same fluorescence band maximum wavelength is observed for the Tyr and Phe background mutants, suggesting similar Trp environments when folded. The fluorescence changes also indicate that urea induces more solvent exposure of W223 in a Tyr background. Thus, $W223_{Tyr}$ towards the cytoplasmic end of helix VII, reveals local unfolding in this region, in accordance with the small reduction in helical content observed for this mutant.

Relative stability of helix I and VII

In a Phe background, W33 on helix I reports a higher local stability than its partner single Trp, F243W, on helix VII in the C domain (see Table 2). W223 also suggests local unfolding at the opposite end of helix VII to F243W. Thus, there are differences in domain stability localised to the vicinity of the first helix of each domain. We provide thermodynamic measures of overall LacY stability as well as that reported at different specific locations across the protein. We can speculate that these fundamental thermodynamic stabilities directly relate to the relative intrinsic stabilities of different regions of the protein *in vivo*. It is possible that an inherent stability of helix I and its immediate structural interactions may play a role in cellular folding providing a stable helix to anchor in the membrane, since helix I is presumably the first helix to fold and emerge from the translocon into the bilayer during co-translational folding of LacY. This is in line with results on the archaebacterial protein bacteriorhodopsin, where helix I of this 7 helical protein inserts first during cellular folding, is structured in the folding transition state, and is inherently stable as an individual helix *in vitro* [30; 32]. Insertion of the second, C domain of LacY does not appear to require the equivalent regions of the domain at the initial helix of the C domain to have enhanced stability. This is despite the fact

that that the C domain can be expressed and folded in the absence of the N domain [32], and that the two domains exhibit pseudo symmetry and are thought to arise from gene duplication [33].

Interestingly, the relative instability associated with the cytoplasmic end of helix VII, compared to the equivalent location on the N domain at the end of helix I, found here *in vitro* also correlates with the influence of native lipids on LacY folding and domain topology during cellular biogenesis. The natural membrane of LacY is dominated by phosphatidylethanolamine (PE) lipids. In *E. coli* strains lacking PE, the whole of the N domain of LacY is inverted in the membrane, which is enabled by helix VII of the C domain acting as a hinge and exiting the membrane; this in turn alters the overall fold of the C domain notably with the loss of packing interactions of helix VII [1; 34]. The relatively low hydrophobicity of helix VII, due to the presence of two negatively charged residues D237 and D240, could contribute to the unpacking of this helix and emergence into the periplasm.

Domain interface and accessibility

The stability of LacY can be increased with mutations at the domain interface that can stabilise a certain conformation, leading to further interactions between the domains and reducing the aqueous accessibility of this region. These stabilising mutations will also reduce access of denaturants such as urea to the domain interface and substrate binding pocket, leading to less denaturation than for the flexible WT protein.

The increased stability of the Tyr mutants stems primarily from mutation of W151 to Tyr; thus WT stability is observed for $W151_{Tyr}$ which retains the native W151. W151 forms part of the substrate binding site at the domain interface in LacY (Fig 1), forming interactions with the substrate via aromatic stacking between the indole of W151 and the sugar galactopyranosyl rings. Fluorescence quenching studies with $F261W_{Tyr}$ and $F261W_{Phe}$ show that the stable Tyr background mutants have lower aqueous accessibility at the domain interface than the less stable Phe mutants. Thus, increased stability correlates with reduced accessibility to the hydrophilic binding site, which is likely to result from reduced interdomain flexibility.

The newly introduced Tyr residue at position 151 in LacY mutant W151Y could stabilise the protein as a result of additional interactions that are absent in native LacY. Initial studies of potential hydrogen bonds involving W151Y across the domain interface suggest that there is a network of interactions or hydrogen bonds. This stabilising network of the new Tyr at position 151 and the native residues E269 andH322 contribute to the increased stability of W151Y, as removing these interactions by mutating E269 and H322 reduces the stabilising effect of W151Y. The effect is complicated however and does not arise from a single bond to E269, since mutating E269 has little effect on W151Y, but nearly eliminates the stabilising effect of W151Y when additional native Trps are mutated to Tyr. Both E269 and H322 are essential for LacY transport and function [35]. E269 is vital to both H^+ translocation and substrate recognition, and H322 for H^+ translocation. A hydrogen bond between W151 and E269 in the binding site has been proposed that could

be altered with Tyr at position 151 as opposed to Trp [36], although in this earlier study the stabilising C154G mutation was also present, which could affect the interactions at the domain interface. The C154G mutation stabilises the protein, locking it in an inward open conformation capable of binding substrate but not of transport [37; 38; 39]. E269Q in conjunction with C154G decreases the stabilising influence of C154G alone.

Conclusions

Measurements of thermodynamic stability are rare for multi-domain α helical proteins. Here we extend our previous measurement of the unfolding free energy of GalP to another member of the MFS, LacY. LacY can be reversibly unfolded enabling the free energy changes associated with recovery of native helical structure and ligand binding activity to be determined. The free energy for the two MFS proteins is very similar, in spite of the high flexibility of LacY. Mutations at the interface of the two domains of LacY increase protein stability by reducing accessibility of the interface to the aqueous surroundings. A single point mutation at the interface of the two domains is sufficient to render LacY resistant to urea denaturation. Single Trp residues provide useful measures of local intrinsic stability across the two domains and reveal an enhanced stability and resistance to urea denaturation at the cytoplasmic end of helix I, compared to the rest of the protein.

Methods

Materials

All reagents were purchased from Sigma-Aldrich or Fisher Scientific UK Ltd, except where specified. All primers were synthesised by Eurofins. All enzymes used and the 1 kb DNA ladder were purchased from New England Biolabs, with the exception of Pfu polymerase which was purchased either from Fermentas (ThermoFisher Scientific), or Promega. <99.5 % DDM was purchased from Generon. All reagents used were of the highest available grade.

PCR mutagenesis

The kanamycin resistance containing plasmid pST-Blue-1 was used as a vector for all the molecular biology in this paper, in Novagen *E. coli* NovaBlue Singles Competent Cells, or One Shot Top10 Chemically Competent *E. coli*. All mutants were made by PCR site directed mutagenesis. To make the single Trp mutants, five Trps were replaced with Phe leaving one native Trp behind. To create the Tyr background single Trp mutants, the first half of the gene (up to residue 762) was synthesised by Eurofins MWG Operon as all six native Trps are in this first half. The synthesised fragment was then subcloned into the second half

of LacY via an AgeI restriction site. The desired Trps were then individually mutated back in to this Tyr background Trp-less DNA. Trp-less LacY DNA was used as a template to create F243W, F261W and L383W with the desired Phe or Tyr background. WT LacY was used as a template to mutate W151 to Tyr, i.e. the five other native Trps were not mutated. The mutations E269Q and H322F were put into the relevant background i.e. W151Y or $W10_{Tyr}$. All the mutations were confirmed by sequencing (Eurofins MWG Operon), and subcloned into a modified pET-28a expression vector containing a C-terminal His10 tag, using XbaI/XhoI restriction sites on either end of the gene.

Protein expression and purification

LacY was expressed in One Shot BL21-AI Chemically Competent *E. coli*, using the kanamycin resistance containing plasmid pET-28a. The cultures were grown at 37 °C in LB media, and induced with 0.1 % arabinose and 1 mM IPTG at an OD_{600} of 0.6 - 0.8 AU. The cells were harvested by centrifugation at 5000 g when growth became stationary. All buffers during purification contained 50 mM sodium phosphate (pH 7.4), 10 % (v/v) glycerol, 10 mM β-mercaptoethanol and 1 mM DDM, with additional components indicated in brackets. As the critical micelle concentration of DDM is increased by urea, a DDM concentration of 1 mM was used throughout to ensure DDM micelles are present at the highest urea concentration of 8 M that was used (Fig S8). Following growth and induction, the cells were cracked by microfluidiser, and the membranes sedimented by centrifugation at 100,000 g at 4 °C for 30 minutes (Beckman Coulter Optima L-80 XP Ultracentrifuge, rotor 70Ti). The pellets were resuspended in 20 ml solubilisation buffer (200 mM NaCl, 20 mM imidazole, 10 mM β-mercaptoethanol, 40 mM DDM, EDTA free protease inhibitor cocktail tablet (Roche Applied Science)) at 4 °C for two hours. The solubilised membranes were spun at 100,000 g at 4 °C for 30 minutes, and the supernatant retained for purification. This was loaded at 1 $ml.min^{-1}$ onto a 1 ml HisTrap HP Ni^{2+} affinity column (GE Healthcare), previously equilibrated in ten column volumes of binding buffer (20 mM imidazole). Following loading, five column volumes of binding buffer was applied to the column to ensure all the protein was bound to the column, and to wash unbound contaminating protein. The column was then washed with fifty column volumes of wash buffer (75 mM imidazole). The protein was eluted directly into a spin concentrator (Amicon Ultra 50 kDa MWCO, Millipore) with ten column volumes of elution buffer (500 mM imidazole). The β-mercaptoethanol concentration was decreased to 2 mM for subsequent steps. Imidazole was then removed by desalting (5ml HiTrap Desalting Column, GE Healthcare), and gel filtration was used to separate LacY monomers from higher order aggregates.

Equilibrium unfolding and refolding

LacY was unfolded and refolded using the same method as previously described [10], with the following modifications; LacY was unfolded for 5 mins, at pH 7.4 and at 25 °C. Either the fluorescence band maximum or CD signal at 222 nm were used for further analysis, and fitted as described [10]. Briefly, the equilibrium

unfolding curve was used to obtain a free energy value, as the higher protein concentration in these experiments increased the signal to noise ratio. The unfolding curve was fitted to a two-state folding equation where the mean residue ellipticity $\theta = \theta_F - \theta_U(\exp(m([\text{denaturant}]-C_m)/RT)/(1+\exp(m([\text{denaturant}]-C_m)/RT)$. θ_F and θ_U are the CD values of the folded and unfolded states (or similarly for the fluorescence data), and C_m is the midpoint where there are equal amounts of folded and unfolded protein. The free energy of unfolding in the absence of denaturant is obtained from the fitted values, where $\Delta G_{u,}^{H_2O} = mC_m$. The non-linear regression was carried out using Grafit software (Erithacus) and the standard error of the best-fit curve calculated from the residuals.

CD spectroscopy

All CD spectra were measured in an Aviv Circular Dichroism Spectrophotometer, Model 410 (Biomedical Inc, Lakewood, NJ USA), with specially adapted sample detection to eliminate scattering artefacts, or at the Karlsruhe synchrotron (UV-CD12 beamline at ANKA, Karlsruhe Institute of Technology). A final protein concentration of 0.1 - 0.5 mg.ml^{-1} was used in quartz rectangular or circular Suprasil demountable cells of pathlengths 0.1 mm, 0.2 mm or 0.5 mm (Hellma Analytics). Each sample was scanned two to four times from 260 - 190 nm, at 1 nm intervals with an averaging time of 0.5 s. Samples containing urea were scanned from 260 - 200 nm due to the high absorbance of urea below 200 nm. The same cell containing buffer only was also measured for background subtraction during data analysis. All CD spectra were processed using CDTool [40], Dichroweb [41] and GraFit. First, the multiple scans were averaged and the buffer background was subtracted. These subtracted spectra were zeroed and smoothed, which set the baseline at zero between 253 - 260 nm. These processed spectra were then imported in to GraFit for further analysis. The data was converted from mdeg to Mean Residue Ellipticity (MRE). The MRE at 222 nm was used for further analysis, by converting it into a percentage of folded protein i.e. 100 % is fully folded protein and 0 % is the amount of secondary structure remaining in 8 M urea. These percentages were then plotted against the urea concentration for comparison between mutants and fitting if appropriate.

ITC measurements of refolded protein

At least 2.5 mg of LacY was unfolded in 8 M urea for 5 minutes, and refolded by a ten times rapid dilution into buffer at 25 °C for 10 minutes, a scale up of the refolding experiments already described. Following the rapid dilution refolding step, the protein was concentrated at 16 °C (Amicon Ultra 50kDa MWCO, Millipore, Megafuge 1.0R centrifuge, Heraeus Instruments) until the protein concentration reached 1 mg.ml^{-1} as determined by the absorbance at 280 nm. The protein was then dialysed in buffer to remove any residual urea, and the same buffer was used to make 800 µM NPG. The ITC experiment was done at 25 °C, with a spacing time of 180 s between injections. All samples were thoroughly degassed before titration. Typically there was a first run of 5 µl and 10 µl injections to a total of 300 µl, followed by a second run of fifteen 20 µl

injections to ensure saturation of the binding sites. A corresponding run of ligand injected into buffer was done to subtract the heat of dilution from the binding heats.

Due to the small amount of heat evolved, it is necessary to adjust the baseline and area of integration of the raw injections, using the adjust baseline tool in the Origin software supplied with the Microcal VP-ITC. This was done for both the protein-ligand and buffer-ligand titrations. A linear fit was applied to the dilution heats of ligand injected into buffer, and this linear fit subtracted from the protein injections. Due to the loss of sample at the tip of the needle during equilibration at the start of each run, the first injection is always wrong and therefore removed from the dataset. As start of the binding isotherm cannot be measured in a low affinity interaction such as this, the stoichiometry of the interaction must be defined in order to fit the data. One and two site binding models both failed to fit the data, so the LacY NPG binding isotherm has been fit with the best fit for the dataset. A sequential model (n=2) was fit to the binding isotherm.

Fluorescence spectroscopy

All fluorescence experiments were recorded with a Fluoromax-2 (ISA Instruments, S.A Inc), using a 4 mm pathlength Starna Quartz cuvette and at a protein concentration of 0.025 $mg.ml^{-1}$. An excitation wavelength of 295 nm was used, with the emission spectrum recorded in 0.25 nm increments from 315-400 nm, and 5 nm bandwidths for both excitation and emission. In all experiments, a scan under identical conditions without protein was also measured, and this background was subtracted from the protein scan. For samples containing urea, an individual scan at each denaturant concentration was required due to its emission peak at 330 nm. The raw fluorescence spectra were imported into GraFit5 (Erithacus), and the relevant background scans were subtracted from each protein scan. Each subtracted spectrum was fitted to an asymmetric peak function to ascertain the wavelength and intensity of the emission band maximum.

Acrylamide quenching

The degree of acrylamide quenching of intrinsic Trp fluorescence was measured as an indicator of solvent accessibility. Fluorescence intensity of each sample in 0 - 0.3 M acrylamide was measured, in 0.5 M steps. A sample containing only buffer was also measured for subtraction of the background fluorescence. The fluorescence intensity at the emission band maximum was used for further analysis. F_o/F_x was plotted against acrylamide concentration, the original fluorescence in absence of acrylamide being F_o, and the fluorescence at each acrylamide concentration being F_X. A linear fit was applied to F_o/F_x, which gave the Stern-Volmer constant, K_{SV}, in M^{-1}.

Acknowledgments

We are very grateful to Ron Kaback for providing LacY plasmids, advice on mutant LacY stability and function as well as comments on the manuscript. This work was funded by the BBSRC (studentship to NJH and research grants BB/F013183/1 and G008833/1 to PJB) and the European Research Council (Advanced Grant 294342 to PJB). PJB also thanks the Royal Society for a Wolfson Research Merit Award and the Leverhulme Trust for a Research Fellowship.

References

1. Vitrac, H., Bogdanov, M., Heacock, P. & Dowhan, W. (2011). Lipids and topological rules of membrane protein assembly: balance between long- and short-range lipid-protein interactions. *J Biol Chem*.
2. Curran, A. R., Templer, R. H. & Booth, P. J. (1999). Modulation of folding and assembly of the membrane protein bacteriorhodopsin by intermolecular forces within the lipid bilayer. *Biochemistry* **38**, 9328-36.
3. Allen, S. J., Curran, A. R., Templer, R. H., Meijberg, W. & Booth, P. J. (2004). Controlling the folding efficiency of an integral membrane protein. *J Mol Biol* **342**, 1293-304.
4. Miller, D., Charalambous, K., Rotem, D., Schuldiner, S., Curnow, P. & Booth, P. J. (2009). In vitro unfolding and refolding of the small multidrug transporter EmrE. *J Mol Biol* **393**, 815-32.
5. Seddon, A. M., Lorch, M., Ces, O., Templer, R. H., Macrae, F. & Booth, P. J. (2008). Phosphatidylglycerol lipids enhance folding of an alpha helical membrane protein. *J Mol Biol* **380**, 548-56.
6. Curnow, P. & Booth, P. J. (2007). Combined kinetic and thermodynamic analysis of alpha-helical membrane protein unfolding. *Proc Natl Acad Sci U S A* **104**, 18970-5.
7. Lau, F. W. & Bowie, J. U. (1997). A method for assessing the stability of a membrane protein. *Biochemistry* **36**, 5884-92.
8. Barrera, F. N., Renart, M. L., Poveda, J. A., de Kruijff, B., Killian, J. A. & Gonzalez-Ros, J. M. (2008). Protein self-assembly and lipid binding in the folding of the potassium channel KcsA. *Biochemistry* **47**, 2123-33.
9. Roman, E. A., Arguello, J. M. & Gonzalez Flecha, F. L. (2010). Reversible unfolding of a thermophilic membrane protein in phospholipid/detergent mixed micelles. *J Mol Biol* **397**, 550-9.
10. Findlay, H. E., Rutherford, N. G., Henderson, P. J. & Booth, P. J. (2010). Unfolding free energy of a two-domain transmembrane sugar transport protein. *Proc Natl Acad Sci U S A* **107**, 18451-6.
11. Huysmans, G. H., Baldwin, S. A., Brockwell, D. J. & Radford, S. E. (2010). The transition state for folding of an outer membrane protein. *Proc Natl Acad Sci U S A* **107**, 4099-104.
12. Boudker, O. & Verdon, G. (2010). Structural perspectives on secondary active transporters. *Trends Pharmacol Sci* **31**, 418-26.
13. Smirnova, I., Kasho, V. & Kaback, H. R. (2011). Lactose permease and the alternating access mechanism. *Biochemistry* **50**, 9684-93.
14. Madej, M. G., Soro, S. N. & Kaback, H. R. (2012). Apo-intermediate in the transport cycle of lactose permease (LacY). *Proc Natl Acad Sci U S A* **109**, E2970-8.
15. Huang, Y., Lemieux, M. J., Song, J., Auer, M. & Wang, D. N. (2003). Structure and mechanism of the glycerol-3-phosphate transporter from Escherichia coli. *Science* **301**, 616-20.
16. Guan, L., Mirza, O., Verner, G., Iwata, S. & Kaback, H. R. (2007). Structural determination of wild-type lactose permease. *Proc Natl Acad Sci U S A* **104**, 15294-8.
17. Yin, Y., He, X., Szewczyk, P., Nguyen, T. & Chang, G. (2006). Structure of the multidrug transporter EmrD from Escherichia coli. *Science* **312**, 741-4.
18. Dang, S., Sun, L., Huang, Y., Lu, F., Liu, Y., Gong, H., Wang, J. & Yan, N. (2010). Structure of a fucose transporter in an outward-open conformation. *Nature* **467**, 734-8.
19. Newstead, S., Drew, D., Cameron, A. D., Postis, V. L., Xia, X., Fowler, P. W., Ingram, J. C., Carpenter, E. P., Sansom, M. S., McPherson, M. J., Baldwin, S. A. & Iwata, S. (2011). Crystal structure of a

prokaryotic homologue of the mammalian oligopeptide-proton symporters, PepT1 and PepT2. *EMBO J* **30**, 417-26.
20. Solcan, N., Kwok, J., Fowler, P. W., Cameron, A. D., Drew, D., Iwata, S. & Newstead, S. (2012). Alternating access mechanism in the POT family of oligopeptide transporters. *EMBO J* **31**, 3411-21.
21. Sun, L., Zeng, X., Yan, C., Sun, X., Gong, X., Rao, Y. & Yan, N. (2012). Crystal structure of a bacterial homologue of glucose transporters GLUT1-4. *Nature* **490**, 361-6.
22. Quistgaard, E. M., Low, C., Moberg, P., Tresaugues, L. & Nordlund, P. (2013). Structural basis for substrate transport in the GLUT-homology family of monosaccharide transporters. *Nat Struct Mol Biol* **20**, 766-8.
23. le Coutre, J., Narasimhan, L. R., Patel, C. K. & Kaback, H. R. (1997). The lipid bilayer determines helical tilt angle and function in lactose permease of Escherichia coli. *Proc Natl Acad Sci U S A* **94**, 10167-71.
24. Abramson, J., Smirnova, I., Kasho, V., Verner, G., Kaback, H. R. & Iwata, S. (2003). Structure and mechanism of the lactose permease of Escherichia coli. *Science* **301**, 610-5.
25. Lau, F. W. & Bowie, J. U. (1997). A method for assessing the stability of a membrane protein. *Biochemistry* **36**, 5884-5892.
26. Curnow, P. & Booth, P. J. (2007). Combined kinetic and thermodynamic analysis of alpha-helical membrane protein unfolding. *Proc Natl Acad Sci U S A* **104**, 18970-18975.
27. Frillingos, S., Sahin-Toth, M., Wu, J. & Kaback, H. R. (1998). Cys-scanning mutagenesis: a novel approach to structure function relationships in polytopic membrane proteins. *Faseb J* **12**, 1281-99.
28. Weitzman, C., Consler, T. G. & Kaback, H. R. (1995). Fluorescence of native single-Trp mutants in the lactose permease from Escherichia coli: structural properties and evidence for a substrate-induced conformational change. *Protein Sci* **4**, 2310-8.
29. Menezes, M. E., Roepe, P. D. & Kaback, H. R. (1990). Design of a membrane transport protein for fluorescence spectroscopy. *Proc Natl Acad Sci U S A* **87**, 1638-42.
30. Curnow, P. & Booth, P. J. (2009). The transition state for integral membrane protein folding. *Proc Natl Acad Sci U S A* **106**, 773-8.
31. Vazquez-Ibar, J. L., Guan, L., Svrakic, M. & Kaback, H. R. (2003). Exploiting luminescence spectroscopy to elucidate the interaction between sugar and a tryptophan residue in the lactose permease of Escherichia coli. *Proc Natl Acad Sci U S A* **100**, 12706-11.
32. Curnow, P., Di Bartolo, N. D., Moreton, K. M., Ajoje, O. O., Saggese, N. P. & Booth, P. J. (2011). Stable folding core in the folding transition state of an alpha-helical integral membrane protein. *Proc Natl Acad Sci U S A* **108**, 14133-8.
33. Reddy, V. S., Shlykov, M. A., Castillo, R., Sun, E. I. & Saier, M. H., Jr. (2012). The major facilitator superfamily (MFS) revisited. *FEBS J* **279**, 2022-35.
34. Bogdanov, M., Xie, J., Heacock, P. & Dowhan, W. (2008). To flip or not to flip: lipid-protein charge interactions are a determinant of final membrane protein topology. *J Cell Biol* **182**, 925-35.
35. Guan, L. & Kaback, H. R. (2006). Lessons from lactose permease. *Annu Rev Biophys Biomol Struct* **35**, 67-91.
36. Vazquez-Ibar, J. L., Guan, L., Weinglass, A. B., Verner, G., Gordillo, R. & Kaback, H. R. (2004). Sugar recognition by the lactose permease of Escherichia coli. *J Biol Chem* **279**, 49214-21.
37. Smirnova, I. N. & Kaback, H. R. (2003). A mutation in the lactose permease of Escherichia coli that decreases conformational flexibility and increases protein stability. *Biochemistry* **42**, 3025-31.
38. Ermolova, N. V., Smirnova, I. N., Kasho, V. N. & Kaback, H. R. (2005). Interhelical packing modulates conformational flexibility in the lactose permease of Escherichia coli. *Biochemistry* **44**, 7669-77.
39. Nie, Y., Sabetfard, F. E. & Kaback, H. R. (2008). The Cys154-->Gly mutation in LacY causes constitutive opening of the hydrophilic periplasmic pathway. *J Mol Biol* **379**, 695-703.
40. Lees, J. G., Smith, B. R., Wien, F., Miles, A. J. & Wallace, B. A. (2004). CDtool-an integrated software package for circular dichroism spectroscopic data processing, analysis, and archiving. *Anal Biochem* **332**, 285-9.
41. Whitmore, L. & Wallace, B. A. (2004). DICHROWEB, an online server for protein secondary structure analyses from circular dichroism spectroscopic data. *Nucleic Acids Res* **32**, W668-73.

Figure Legends

Figure 1- Positions of Trp reporters in LacY

The location of each single Trp reporter is highlighted. The corresponding pairs of Trps on each domain have been coloured the same; W10 and W223 are orange, W33 and F243W are green, W171 and L383W are purple and F261W and W151 are red. W78 is coloured cyan and does not have a partner in the opposite domain. **A** LacY is shown perpendicular to the membrane, with the N domain on the right, the C domain on the left, and the cavity open towards the cytoplasm. **B** The view of LacY from the periplasm, with the C domain on the left. In A and B helices I and VII have been highlighted in blue. These figures were made in PyMOL (v 0.99, DeLano Scientific) using PDB file 2V8N. **C** Simplified cartoon of Trp positions in LacY. W10, W33, W151, W223, F243W, F261W have been highlighted with larger text.

Figure 2- Refolding of WT LacY reported by CD spectroscopy

A. Folded WT LacY was incubated in DDM (solid black line) and or 8 M urea (solid red line) for 5 min at room temperature. The latter was diluted into DDM for 10 mins, giving refolded LacY (dashed green line). Residual urea was removed from the refolded LacY sample by binding to Ni-NTA beads, followed by protein elution with 200 mM imidazole, which was removed by dialysis (solid blue line). Deconvolution of this spectrum estimated the α helical content as 83 % helix i.e. the native amount of helicity. **B** Unfolding (open circles) and refolding (black circles) of WT LacY measured by CD intensity at 222 nm. The amount of folded protein was determined from the degree of α helical structure as measured by the CD intensity at 222 nm, and the resulting values normalised between 0 % and 100 %. The latter represents the fully folded protein in DDM (with 85 % helix) and the former 0 % represents the urea-unfolded state that is partly structured (with approximately 55 % helix, see Fig 2A). The solid line represents a two state fit to the unfolding data. Unfolding was measured in a 0.2 mm pathlength cell at 0.15 – 0.24 mg.ml^{-1} LacY, with each data point being the result of twelve repeats giving a mean SE for the two state fit of ±9.64 %. Refolding was measured at 0.05mg.ml^{-1} LacY in a 0.5mm pathlength cell, and data points are the result of six repeats with a mean SE of ±10.9 %. The SE for data at 1M urea was ±4 %.

Figure 3– Unfolding of single Trp mutants $W33_{Phe}$, $W33_{Tyr}$, $F243W_{Phe}$ and $W223_{Phe}$

A CD spectra for Phe background mutants $F243W_{Phe}$ (left panel) and $W33_{Phe}$ (right panel) folded in DDM (black line) and unfolded in 8 M urea (red line). Spectra for the Tyr background mutant $W33_{Tyr}$ are also shown: in DDM (solid blue line) and 8 M urea (dashed red line). $F243W_{Phe}$ was measured at a concentration of 0.15 mg.ml^{-1}, $W33_{Phe}$ at 0.3 mg.ml^{-1} and $W33_{Tyr}$ at 0.13 mg.ml^{-1}. **B** Fluorescence-derived unfolding and refolding curves from the urea dependence of the intrinsic Trp fluorescence bands. Left panels show changes in the Trp fluorescence band maximum with urea, during unfolding (open circles) and refolding

(filled circles) for F243W$_{Phe}$ (top panels) and W223$_{Phe}$ (bottom panels). The urea dependence of the intrinsic Trp fluorescence band maximum for W33$_{Phe}$ (triangles) is shown for comparison with F243W$_{Phe}$. A positive wavelength shift indicates a red-shift of the band to longer wavelengths, and the solid lines show 2 state fits to the unfolding data. The wavelength band shifts are calculated by setting the wavelength of the fluorescence emission band maximum at 0 M urea to 0. Right panels show linear free energy relationships for ΔG_U with urea concentration. Error bars are the result of two repeat experiments for F243W$_{Phe}$, three repeats experiments for W223$_{Phe}$ and four repeat experiments for W33$_{Phe}$. Protein concentration was 0.025 mg.ml^{-1} for each mutant. Schematic diagrams of the mutant proteins are shown in each case, with the two domains shown in blue and the approximate position of the single Trp indicated by a green circle for the pair W33 and F243W, and an orange circle for W223.

Figure 4 - Stabilising mutations as domain interface

A Secondary structure change in 8 M urea of W151Y**.** W151Y at 0.12 mg.ml^{-1} was incubated in 8 M urea and measured by CD to assess any change in structure. Native W151Y is shown in black, and W151Y in 8 M urea in red. **B** Quenching the intrinsic Trp fluorescence of F261W$_{Phe}$ and F261W$_{Tyr}$**.** Acrylamide quenching of F261W was measured in a Tyr and Phe background. F261W lies on the C domain, at the domain interface opposite W151. F261W$_{Phe}$ is shown in open circles and F261W$_{Tyr}$ in black circles. The gradient of the linear fit gives the K_{sv}, 1.67 ± 0.11 M^{-1} for F261W$_{Phe}$ and 0.52 ± 0.06 M^{-1} for F261W$_{Tyr}$. Errors are taken from the standard error of the linear fit, and error bars are the result of three repeats. Schematic diagrams of the mutant proteins are shown in each case, with the two domains shown in blue. The approximate positions of the Trps and the W151 Tyr mutation are labelled in green and red respectively, and the single Trp F261W indicated by a red circle.

Figure 5 - Domain interface mutations

A The domain interface mutations: C154G, W151Y, F261W, T265V, E269Q and H322F. This figure was made in PyMOL (v 0.99, DeLano Scientific) using PDB file 2V8N. The newly introduced residues are shown using the mutagenesis tool in PyMOL. **B** CD spectra for W10$_{Tyr}$/E269Q, whereall Trps are mutated to Tyr except W10. The folded state is shown by the black line, and unfolded in 8 M urea by the red line. In the accompanying schematic, the location of mutation E269Q is shown by a red star, and the locations of the native Trp W10 and the Tyr mutations have been labelled in green and purple respectively. **C** Schematic of locations of domain interface mutations, with the Trps labelled in green, and the domain mutations labelled in purple. **D** Mutation of potential hydrogen bonding partners of W151, H322F and E269Q, have limited effect on stability. CD spectra of W151Y/E269Q folded (solid black line) and unfolded in 8 M urea (solid red line), compared with W151Y/H322F folded (blue short dashes), and unfolded in 8 M urea (green long dashes). There is a small decrease in the amplitude of the peak at 222nm, but neither mutation

significantly destabilises W151Y. Note that in **A-C** these the N domain on the left and the C domain on the right.

Table 1

The ΔG_U^{H2O} values for WT and the Phe background single Trp mutants, derived from fluorescence and CD denaturation curves

ΔG_U^{H2O} values are determined from the red-shift observed in the Trp fluorescence band upon unfolding in urea, both by a two state fit to the denaturation curve as well as from linear extrapolation of ΔG_U at different urea concentrations. Values determined from CD denaturation curves are shown for comparison for WT LacY, as well as those mutants with sufficient high expression to obtain the larger amounts of protein and higher concentrations necessary for CD denaturation curves. There is good agreement between the fluorescence and CD-derived values. Errors are from the standard error of the fit.

Table 2

Single Trp mutant pairs which exhibit contrasting behaviour with respect to the local structurela environment of helices I and VII, as well as the domain interface, together with key findings. The single Trps which are in a hydrophobic environment in the folded structure are highlighted in grey.

Relative domain folding and stability of a membrane transport protein

Nicola J Harris, Heather E Findlay, John Simms, Xia Liu and Paula J Booth

School of Biochemistry, University of Bristol, Bristol BS8 1TD UK

Correspondence:

Paula J Booth

School of Biochemistry, School of Medical Sciences, University of Bristol, University Walk, Bristol BS8 1TD UK

Tel: +00 44 (0)117 33 12138, Fax: +00 44 (0)117 33 12168, Email: paula.booth@bristol.ac.uk

Abstract

There is a limited understanding of the folding of multidomain membrane proteins. Lactose permease (LacY) of *Escherichia coli* is an archetypal member of the major facilitator superfamily of membrane transport proteins, which contain two domains of six transmembrane helices each. We exploit chemical denaturation to determine the unfolding free energy of LacY and employ Trp residues as site specific thermodynamic probes. Single Trp LacY mutants are created with the individual Trps situated at mirror image positions on the two LacY domains. The changes in Trp fluorescence induced by urea denaturation are used to construct denaturation curves from which unfolding free energies can be determined. The majority of the single Trp tracers report the same stability and an unfolding free energy of ~ +2 kcal.mol^{-1}. There is one exception; the fluorescence of W33 at the cytoplasmic end of helix I on the N domain is unaffected by urea. In contrast, the equivalent position on the first helix, VII, of the C terminal domain exhibits wild type stability, with the single Trp tracer at position 243 on helix VII reporting an unfolding free energy of +2 kcal.mol^{-1}. This indicates that the region of the N domain of LacY at position 33 on helix I has enhanced stability to urea, when compared the corresponding location at the start of the C domain. We also find evidence for a potential network of stabilising interactions across the domain interface, which reduces accessibility to the hydrophilic substrate binding pocket between the two domains.

Keywords

Major facilitator superfamily; thermodynamics; single tryptophan residues; chemical denaturation; folding free energy

Abbreviations

CD, Circular Dichroism; DDM, *n*- dodecyl β-D- maltoside; DOPE, L-α-1,2-dioleoylphospatidylethanolamine; DOPC, L-α-1,2-dioleoylphospatidylcholine; ITC, Isothermal titration calorimetry; GalP, *Escherichia coli* galactose transporter; LacY, Lactose Permease; MFS, Major Facilitator Superfamily; NPG*, p*-nitrophenyl-α-D-galactopyransoside PE, phosphatidylethanolamine; PG, phosphatidylglycerol; SDS, Sodium Dodecyl Sulphate, WT, wild type.

Introduction

Integral membrane proteins adopt diverse structures with differing stability and flexibility as well as numbers of domains or subunits. How much of their protein structure is dictated by the amino acid sequence and how much by the surrounding membrane, additional proteins or other biological factors is largely unknown. Nonetheless, data is accruing on membrane protein folding, ranging from *in vitro* stability and mechanism to co-translational insertion of transmembrane helices and the influence of the surrounding lipids [1; 2; 3; 4; 5]. Sophisticated thermodynamic, kinetic, and structural detail can at present only be derived from *in vitro* study in artificial conditions such as detergents or simplified membranes. Quantitative data on the intrinsic thermodynamic stability of membrane proteins *in vitro* has engendered considerable interest but has only been determined in a few cases [6; 7; 8; 9; 10; 11]. Equally there are few studies of multi-domain protein folding [9; 10], and important questions relating to the stability and cooperativity of the domains are yet to be addressed. Here, we investigate the folding *in vitro* of a flexible, two-domain transport protein, continuing our studies of the most widespread membrane transporter families, the Major Facilitator Superfamily (MFS). This family comprises approximately 25 % of prokaryotic transport proteins and is also prevalent in eukaryotes, notably as sugar transporters [12].

Protein structure within the bilayer falls into two general types: β-barrels and α-helical bundles. We focus on the considerably more abundant latter class of helical proteins that reside in plasma membranes and bacterial inner membranes, where they perform a wide variety of roles as receptors and transporters as well as being directly involved in photosynthesis and ATP production. The nature of their protein scaffold of inherently stable, hydrophobic helices makes them challenging to study. Reversible unfolding has only been demonstrated for a few α-helical membrane proteins [6; 7; 8; 9], but it has proved possible to establish a thermodynamic equilibrium *in vitro* for an MFS protein and determine the free energy for the final folding step, when native ligand binding is recovered [10].

The majority of MFS transporters have 12 transmembrane helices arranged in 2 domains with a substrate binding site located at the domain interface. The binding site seems to be accessible alternately to either side of the membrane, with an apo-intermediate conformation containing an occluded cavity proposed for LacY [13; 14]. The structure of several MFS proteins have been solved to high resolution [15; 16; 17; 18; 19; 20; 21; 22], including the lactose transporter LacY. WT LacY is highly dynamic as shown by the 85-90 % of backbone amide hydrogens exchanging with solvent in < 5 mins in a 3:1 ratio of phospatidylethanolamine (PE) to phosphatidylglycerol (PG) [23]. Crystal structures have been resolved for WT LacY as well as a stable C154G mutant, which binds but does not transport substrate [24]. Both structures are for a conformation with the binding pocket open to the cytoplasm, whilst there are examples of outward open and occluded states amongst the other MFS structures.

Mechanistic folding studies of α helical membrane proteins have been dominated by investigations *in vitro* on the stable, single domain bacteriorhodopsin protein [6]. Thermodynamic measurements have also been achieved for a few other proteins, including bacterial diacylglycerol kinase [7] and the potassium channel KcsA [8]. Recently, we extended the approach to the MFS galactose transporter GalP, of *E. coli*. GalP was reversibly unfolded in DDM micelles by urea, enabling the unfolding free energy to be determined [10]. Moreover, as shown previously for membrane proteins [25; 26], a linear free energy relationship was observed with urea concentration which allows extrapolation to an unfolding free energy, ΔG_u^{H2O} of +2.5 kcal.mol^{-1} in the absence of urea. This provides a reference intrinsic stability measure to quantify stability at specified sites via the change induced in this free energy; $\Delta\Delta G_u^{H2O}$, by a site-directed mutation. GalP loses about a third of its helical structure in 8 M urea, which we suggested was most likely due to urea denaturing helical structure that extends beyond the membrane as well as via the hydrophilic substrate binding pocket between the two domains. Unfortunately the structure of GalP has yet to be solved, hence we translate the approach to the extremely well studied lactose transporter of *Escherichia coli*, LacY, for which results can be interpreted in the context of a known high resolution structure. We exploit the ΔG_u^{H2O} measurement to probe the relative stability at specific sites of the two transporter domains as well as at the domain interface. We combine free energy measurements with site-specific mutagenesis and use single Trp reporters of local thermodynamic stability. LacY has been extensively mutated with only 6 residues in the protein being absolutely required for function, none of which are a Trp [27]. LacY contains 6 native Trp residues, and single Trp mutants of LacY have previously been prepared where the remaining 5 native Trps have been mutated either all to Phe or all to Tyr [28; 29]. Transport activities of these single Trp mutants are 75-100 % of WT LacY, regardless of whether Phe or Tyr is used as the Trp replacement [29]. Replacing native Trps with Tyr resulted in higher overexpression.

Our strategy is to use unique Trp residues to probe particular regions of the protein. This approach assesses the local structural and solvent environment of each Trp, building up a picture of stability across the two domains. For these experiments, we created two series of single Trp mutants. Firstly, the 6 native Trp residues of LacY were all mutated to Phe to give a Trp-less LacY mutant with a Phe background. Additionally, all native Trps were mutated to Tyr, giving Trp-less, Tyr background LacY. Into these Trp-less backgrounds a single Trp was introduced at a specified site. The sites chosen are shown in Fig 1. Firstly we used the locations of the 6 native Trps (positions 10, 33, 78, 151, 171 and 223) and re-introduced individual native Trps into the Phe and Tyr backgrounds. This generated two versions of the same single Trp mutant: one in a Phe background (where all other native Trps are mutated to Phe) and one in a Tyr background (where all other native Trps are mutated to Tyr). We denote the backgrounds with a subscript; thus $W33_{Phe}$ and $W33_{Tyr}$ refer to the single Trp W33 in a Phe or Tyr background respectively, with a Trp at position 33 in the protein. Each of the native LacY Trps is in a different environment (see Fig 1), either buried within the helical bundle, in the hydrophilic binding pocket or surface exposed to lipids. Thus the native Trp positions

report on a number of different locations across the protein. However, the native Trps are primarily located in the N domain of LacY, with only one in the C domain. We therefore created additional single Trp mutations with non-native Trps introduced into the C domain, at positions that mirrored those of the native N domain Trps. These non-native single Trp mutants are designated by the mutation, using a subscript to denote the Phe or Tyr background. Again two versions of each non-native single Trp were made; $F261W_{Phe}$ and $F261W_{Tyr}$ thus refer to the single Trp mutant F261W in a Phe or Tyr background respectively, with a Trp at position 261 introduced by mutation of F261. Additionally, we quote in brackets the domain and helix location of the single Trp together with its local environment. Thus position 243 is on helix VII in the C domain at an interhelical position, which we refer to as: $F243W_{Phe}$ (C domain helix VII; interhelix). This array of single Trp mutants allows us to compare intrinsic stability at equivalent structural sites on the two domains of LacY. We use Trp fluorescence to follow changes in the local structure induced by urea denaturation, together with far UV circular dichroism (CD) to monitor the changes in the overall protein secondary structure content. Additionally, we use aqueous fluorescence quenchers of Trp residues in the binding site to correlate binding pocket accessibility with urea stability for stabilising mutations at the domain interface.

Results

Reversible unfolding of LacY

Equilibrium chemical denaturation provides a useful method for free energy determination. LacY in 1 mM dodecylmaltoside (DDM) was reversibly denatured by urea, as previously shown for GalP [10]. Far UV CD showed the same, ~30 %, reduction in WT LacY α helical structure (with all native Trps present) in 8 M urea as for GalP (as estimated from the reduction in the negative band intensity at 222 nm indicative of α helical structure; see Fig 2A). The 8 M-urea denatured state of LacY (and GalP) thus contains ~70 % of the native helical structure. Such structured, chemically-denatured states are usual for transmembrane helical proteins since denaturants such as urea or SDS do not fully unfold transmembrane helices. Upon refolding LacY from 8 M urea, by dilution into DDM detergent micelles, the far UV CD spectrum returned to that of the original purified native protein. Isothermal titration calorimetry (ITC) binding measurements with the lactose analogue, *p*-nitrophenyl-α-D-galactopyransoside (NPG) demonstrate that native binding activity returns once the protein has refolded, with a K_d of 93 µM, compared to the original, folded WT K_d of 10 µM (see Fig S1).

Equilibrium denaturation curves were determined as reported previously for GalP [10], by incubating originally folded LacY (in DDM) in increasing concentrations of urea (see Fig 2B). The refolding curve was generated by first unfolding LacY in 8 M urea, then refolding by dilution into different urea concentrations.

As found previously for GalP, the folding and unfolding curves overlay, which is consistent with a reversible reaction. Assuming the simplest model, the data were fit to a two-state reaction (Fig 2B), which is also in line with the previous report on GalP. Partially unfolded LacY was more prone to aggregation than GalP at high urea concentrations (> 6 M), which affected the CD data quality especially for refolding data for which signal to noise is lower as a result of lower protein concentrations. The higher quality unfolding data were fit to a two-state equation, giving an unfolding free energy in the absence of urea, ΔG_u^{H2O}, of +2.7 ± 0.6 kcal.mol^{-1} at pH 7.4. The free energy of unfolding, ΔG_u was also calculated at different urea concentrations and found to be linear with urea concentration, giving a ΔG_u^{H2O} of +2.5 kcal.mol^{-1} by extrapolation to zero urea (see Fig S2). These ΔG_u^{H2O} values for LacY are very similar to that obtained for GalP, of ΔG_u^{H2O} of + 2.5 kcal.mol^{-1} (at pH 8 [10]).

Single Trps as site-specific reporters of stability

The 6 native Trps of LacY complicate the fluorescence spectra of the wild type protein and changes therein upon unfolding. Thus we employ single Trp mutants. Far UV CD spectra showed that the secondary structure of all the single Trp mutants in a Phe background exhibited similar stability to urea as WT LacY, with an approximately 30 % reduction in secondary structure in 8 M urea (Fig 3A and Fig S3). The apparent spectral shape changes for certain Trp mutants arise from lower signal to noise for the data from mutant LacY proteins for which lower expression and protein concentrations was found. This issue of lower quality spectra is more pronounced for the urea-denatured state as the presence of urea also reduces spectral quality and the characteristic α helical CD signal at 222 nm is smaller. Since the urea-denatured state is partly structured it is possible that the Trp mutations induce alterations in this unfolded state, an issue previously discussed for helical membrane protein unfolding investigations [30]. However, it is not possible to conclude that the urea-denatured states of the mutants have different secondary structure from these CD spectra.

The changes in single Trp fluorescence were monitored during urea-induced unfolding and refolding. Trp fluorescence of all but one single Trp ($W33_{Phe}$) in a Phe background decreased in intensity and shifted to longer wavelengths upon urea denaturation. No change in fluorescence was observed for $W33_{Phe}$ (N terminal helix I, interhelix; Fig 3B (top left) and Table S1). For these unfolding measurements, the red shift in the fluorescence emission band was used as a measure of unfolding. Using the fluorescence intensity to mmoitor unfolding was unreliable and irreproducible due to the formation of dimers and aggregates at higher urea concentrations (Fig S4). The increase in the wavelength of the emission band maximum with increasing urea concentration is indicative of increased Trp exposure to hydrophilic or polar solvents and therefore monitors unfolding. The wavelength of the fluorescence band maxima for each single Trp mutant differ in the folded and urea states, illustrating their different solvent exposure and environment (see Table S2). Urea-denaturation curves were generated from the change in the wavelength of the fluorescence band

maxima against urea concentration (Fig 3B, Fig S5). Upon refolding, the original fluorescence wavelength was recovered for each single Trp and the refolding curves overlaid the unfolding curves, showing reversible unfolding as indicated by CD for WT LacY (Fig 2B). This enabled ΔG_U^{H2O} values to be determined from the fluorescence denaturation curves. The fluorescence-derived curves could be fit with a two state, equilibrium reaction. ΔG_U^{H2O} values were obtained either from the fit to the denaturation curve, or by evaluating the equilibrium constant for the assumed two-state reaction, and thus ΔG_U, at different urea concentrations and extrapolating to zero urea, as described previously [6; 10]. Fig 3B shows the latter linear free energy plots for $F243W_{Phe}$ and $W223_{Phe}$ (both on C domain helix VII). ΔG_U^{H2O} values were determined for the Phe background single Trp mutants and found to be similar to the WT LacY ΔG_U^{H2O} of +2.5 kcal.mol^{-1} determined from CD data (see Table 1). For example, ΔG_U^{H2O} for $F243W_{Phe}$ and $W223_{Phe}$ were +2.2 kcal.mol^{-1}. From these two-state fits an unfolding transition midpoint, Cm, is also derived, for which the values are also found to be similar for both WT and the single Trp mutants (Table S3). The gradient, m_U^{H2O}, characterising the linear dependence of ΔG_U on urea (for example as shown in Fig3B) was also found to be similar for the Trp mutants (Table S3). This analysis of the single Trp fluorescence data gives a local thermodynamic measure of stability because it is determined from a site-specific reporter.

Table 2 summarises results of single Trp pairs that exhibited differing behaviour, giving insight into relative domain stability and resistance to urea denaturation. The only pair of Trp mutants to exhibit differing degrees of unfolding in chemical denaturants, when measured by intrinsic Trp fluorescence, is that on the first helix of each domain. The Trp fluorescence of $W33_{Phe}$, on helix I of the N domain is unchanged by urea indicating resistance of the local protein structure to urea denaturation. In contrast, the equivalent C domain single Trp $F243W_{Phe}$ on helix VII exhibits the same urea-induced fluorescence changes and thus local unfolding as the other single Trp mutants studied (Fig 3B and Table 2). W33 is a native Trp, but F243W is a new Trp introduced at position 243 on the C domain through mutation of Phe. The introduction of this non-native Trp in $F243W_{Phe}$ does not however affect the overall protein stability with respect to secondary structure denaturation by urea, which is the same as for both W33 and WT LacY (Fig 3A). Thus, the Trp fluorescence changes of $W33_{Phe}$ and $F243W_{Phe}$ report upon the local Trp environment. The aqueous accessibility of $W33_{Phe}$ and $F243W_{Phe}$ in the folded protein was assessed by exposure to acrylamide quenching of Trp fluorescence. The two Trps had similar Stern-Volmer constants (K_{SV}); K_{sv}, 1.76 ± 0.07 M^{-1} for W33 and 1.48 ± 0.12 M^{-1} for F243W (Fig S6). $W33_{Phe}$ and $F243W_{Phe}$ therefore have similar accessibility to urea in the folded state and exhibit similar overall secondary structural loss in urea, but have different Trp fluorescence changes.

Stable, single Trp mutants in a Tyr background

The single Trp mutants were also made with a Tyr, as opposed to Phe, background. All but one single Trp mutant with a Tyr background showed an increased stability to urea denaturation over both WT and the

Phe background counterparts, with little or no reduction in secondary structure in 8 M urea (Fig S3). W151 (N domain, helix V, domain interface) was the only single Trp mutant to show a similar, WT, reduction in secondary structure in both a Phe and Tyr background.

$W223_{Tyr}$ is at the cytoplasmic end of the first helix of the C domain, helix VII. The secondary structure of this Tyr background mutant, $W223_{Tyr}$, was more stable to urea denaturation than the Phe background equivalent, $W223_{Phe}$. The far UV CD spectra of $W223_{Tyr}$ showed a smaller reduction in the intensity of the negative 222 nm band indicative of helical structure (Fig S7). In contrast to all other Tyr background mutants, including its partner $W10_{Tyr}$ on helix I, $W223_{Tyr}$ has a larger red shift in fluorescence than its Phe background equivalent, $W223_{Phe}$ upon urea denaturation. This suggests greater local unfolding in this cytoplasmic region of helix VII (see Table 2 and Fig S7). The fluorescence emission bands of folded and urea-denatured $W223_{Tyr}$ states were also blue shifted to lower wavelengths by 14 nm and 11 nm, respectively, relative to the folded and unfolded state of $W223_{Phe}$ (Fig S7 and table S4). These large blue-shifts suggest that W223 in a Tyr background is in a more non-polar environment, with a decreased aqueous exposure, than W223 in a Phe background. These variations in the fluorescence spectra of $W223_{Tyr}$ and $W223_{Phe}$ suggest slightly different behaviour of the Tyr background mutant $W223_{Tyr}$ to the other single Trps reported here, with local changes in the vicinity of position 223 on helix I being different in a Tyr as compared to a Phe background. The fluorescence denaturation curve of $W223_{Tyr}$ is also different in that it does not plateau at high urea concentrations. Thus it is not possible to fit a two-state reaction and determine the ΔG_U^{H2O} for $W223_{Tyr}$.

Domain interface

All single Trp mutants were more stable to urea denaturation in a Tyr than in a Phe background, except $W151_{Tyr}$ on the N domain at the domain interface. $W151_{Tyr}$ contains a Trp at position 151 in the domain interface, with all other native Trps mutated to Tyr. In all the other single Trp, Tyr background mutants W151 is mutated to Tyr. We therefore investigated whether a single Trp to Tyr mutation at this position, W151Y, could be responsible for the increased Tyr background stability. The mutant W151Y has only the Trp at position 151 substituted by Tyr with the other five native Trps being present. W151Y was found to be more stable with respect to urea denaturation of secondary structure than both WT and $W151_{Tyr}$, which is consistent with the single Trp to Tyr change at 151 being primarily responsible for the increased stability of the Tyr background mutants. W151Y was resistant to urea denaturation, with no reduction in secondary structure (Fig 4A) in line with the Tyr background mutations. W151 lies at the domain interface (Fig 1) and the aqueous accessibility of this interface was probed by acrylamide quenching of Trp fluorescence. The aim was to assess aqueous accessibility of a Trp at this interface in a more stable (i.e. Tyr background) and less stable (i.e. Phe background) mutant. Since W151 has the same stability in both a Tyr and Phe background, quenching of the single Trp mutant F261W was measured. F261W lies at the domain interface

on the C domain, but in a mirror image position to the N domain W151. F261W can be used to illustrate the difference in quenching with stability, since F261W also has increased stability in a Tyr background over a Phe background (Fig S3). The Trp at position 261 showed less quenching in the more stable Tyr background ($F261W_{Tyr}$) than Phe ($F261W_{Phe}$), with K_{SV} values of 0.52 ± 0.06 M^{-1} and 1.67 ± 0.11 M^{-1} respectively, indicating a lower exposure of Trp to acrylamide in the Tyr background (Fig 4B). The K_{SV} value of $F261W_{Phe}$ corresponds well with that previously published for $W151_{Tyr}$ of 2.01 ± 0.1 M^{-1} [31], indicating similar accessibility of $W151_{Tyr}$ to the Phe single Trp mutants.

Additional hydrogen bonds involving the newly introduced Tyr at position 151 were investigated as a possible cause of the increased stability of W151Y. Potential hydrogen bonding partners of W151Y across the domain interface were deleted (Fig 5A); T265, E269 and H322, and the stability of double mutants, which contained one of these deletions combined with W151Y, were measured. If hydrogen bonding is a factor, these deletion mutants should be less stable than W151Y. The potential hydrogen bonding partner mutations were also incorporated into the single Trp $W10_{Tyr}$, to measure them in a Tyr background. Thus for example $W10_{Tyr}$/E269Q lacks a possible E269-W151Y interaction as well as having all native Trps replaced by Tyr, except W10. E269 is important for LacY transport and for these initial investigations of interactions across the domain interface, a conservative mutation with respect to size was made. E269 was mutated to a residue of similar size, Gln, despite the fact that the newly introduced residue could introduce new interactions from the Gln amide group. T265V had no effect on stability, whilst the double mutants W151Y/H322F and W151Y/E269Q were slightly less stable than W151Y (see Fig 5D). $W10_{Tyr}$/E269Q was the only mutant studied to have decreased stability, with a significant reduction in helicity in urea (Fig 5B), although this mutant could not be refolded, and thus showing irreversible denaturation of $W10_{Tyr}$/E269Q. LacY with all Trp mutated to Tyr is also slightly less stable than W151Y, thus the reduction in stability of $W10_{Tyr}$/E269Q compared to W151Y is due both to the additional native Trp-Tyr mutations (i.e. as present in $W10_{Tyr}$), as well as hydrogen bond or other interactions that are affected by E269Q and H322F. E269Q also reduced the stability of C154G; a stabilising mutation in the domain interface.

Discussion

Site-specific reporters across LacY reveal that the two domains exhibit similar thermodynamic stability, apart from in the region of the first helix of each domain. The fluorescence emission of each single Trp depends upon the local solvent environment of the Trp residue in question. Hence, the Trps in different positions on the folded protein exhibit different wavelengths for the positions of their fluorescence band maxima, reflecting their contrasting environments (Table S2). The individual Trps studied here therefore report on local changes in the protein structure and solvent surroundings at the location of the Trp. The separate Trps also exhibit differing shifts in the position of their emission maxima upon urea denaturation,

again showing their sensitivity to changes in the local environment. However, the unfolding transitions these shifts measure (apart from W33) are remarkably similar, revealing comparable unfolding free energies, analogous dependence upon urea and in turn equivalent thermodynamic stability at zero urea. This strongly implies that at each site studied on LacY (apart from position 33) the apparent unfolding free energy is similar. Moreover, these thermodynamic values reported by the change in position of the fluorophore emission bands concur with those determined from changes in CD spectra. The latter reports upon the overall reduction in protein secondary structure upon urea denaturation. Thus the individual thermodynamic stabilities reported by the single Trps at sites across the protein are the same as the global thermodynamic stability of the protein, determined from CD spectra. This suggests cooperative unfolding of LacY. Of the single Trps investigated only one at position 33 of LacY gives different results. Although the same overall reduction in secondary structure as WT occurs upon urea denaturation for $W33_{Phe}$, there is no change in the fluorescence emission band of the Trp. Thus, there is no change in protein structure induced by urea in this region of LacY and therefore the structure of the protein in the vicinity of position 33 on helix I remains structured in the urea-denatured state. The protein structure at this site on the N domain (position 33) is more stable to urea denaturation than the corresponding position on the C domain (position 243). W33 is buried within the helical bundle of the N domain on helix I; hence W33 reports an enhanced local structural stability and resistance to urea denaturation compared to the equivalent position 243 on helix VII in the C domain (see Fig 1). The unfolding free energy reported by $F243W_{Phe}$ is similar to WT and the other single Trp mutants. Additionally, the fluorescence data from the Tyr background mutant $W223_{Tyr}$ suggests local unfolding at the cytoplasmic end of helix VII, in contrast to the corresponding position, $W10_{Tyr}$, on helix I. Thus, the intrinsic stability of the N domain in the region of helix I is greater than that of helix VII, with the structure in the locale of positions 243 and 223 on helix VII being more susceptible to unfolding by urea. Across the rest of the protein individual Trp residue pairs, in a Phe background, at mirror image locations on the N and C domains all report the same unfolding free energy as WT; these include Trps at positions 10, (N, helix I), 78 (N, helix III) and 223 (C, helix VII) all near the cytoplasmic loops on each domain; 151 (N domain, helix V) and 261 (C domain helix VIII) at the domain interface, as well as 171 (N domain helix VI) and 383 (C domain helix XII) facing the detergents or lipids (Fig 1).

Single Trp reporters of local unfolding

The unfolding free energies are determined from urea denaturation curves, with extrapolation to ΔG_u^{H2O} in the absence of urea, as determined previously for the MFS protein, GalP [10]. These are thus intrinsic thermodynamic stability values independent of urea concentration. Denaturation curves obtained from the reduction in secondary structure, as determined by far UV CD, for all single Trp mutations with native Trps mutated to Phe (including $W33_{Phe}$ and $F243W_{Phe}$) are consistent with WT LacY and GalP unfolding free energies of ~ +2 kcal.mol^{-1}. Trp fluorescence-derived curves also give unfolding free energies of ~ +2 kcal.mol^{-1} for all single Trp, Phe background mutants, except $W33_{Phe}$, for which there is no change in W33

fluorescence. Therefore no thermodynamic information can be gained from the fluorescence data with regard to $W33_{Phe,}$ although the results show that the protein structure in the region of position 33 on helix I is resistant to urea denaturation. Both W33 and F243W are equally accessible to aqueous phase fluorescence quenchers in their folded states. Thus the Trp fluorescence band change and unfolding free energy of $F243W_{Phe}$ upon urea denaturation, and lack of for $W33_{Phe}$, report upon the local Trp environment. Whilst far-UV CD derived denaturation, reflecting the overall reduction in secondary structure in urea, is the same for both $W33_{Phe}$ and $F243W_{Phe}$, the single Trp fluorescence denaturation curves from the W33 reporter reveals that this region of the protein is more resistant to urea denaturation than the corresponding region on the C domain, reported by F243W. The Trp fluorescence changes report alterations in both secondary and tertiary structure.

Mutating the native Trps of LacY to Tyr resulted in single Trp mutants that were more stable than WT LacY and the corresponding Phe background mutants, except for $W151_{Tyr}$ at the domain interface, which had similar stability to $W151_{Phe}$ and WT (Fig S3). Additionally, $W223_{Tyr}$ contrasts with the other single Trp, Tyr background mutants in that the fluorescence band suggests $W223_{Tyr}$ is in a more non-polar environment than $W223_{Phe}$. In all other cases studied the same fluorescence band maximum wavelength is observed for the Tyr and Phe background mutants, suggesting similar Trp environments when folded. The fluorescence changes also indicate that urea induces more solvent exposure of W223 in a Tyr background. Thus, $W223_{Tyr}$ towards the cytoplasmic end of helix VII, reveals local unfolding in this region, in accordance with the small reduction in helical content observed for this mutant.

Relative stability of helix I and VII

In a Phe background, W33 on helix I reports a higher local stability than its partner single Trp, F243W, on helix VII in the C domain (see Table 2). W223 also suggests local unfolding at the opposite end of helix VII to F243W. Thus, there are differences in domain stability localised to the vicinity of the first helix of each domain. We provide thermodynamic measures of overall LacY stability as well as that reported at different specific locations across the protein. We can speculate that these fundamental thermodynamic stabilities directly relate to the relative intrinsic stabilities of different regions of the protein *in vivo*. It is possible that an inherent stability of helix I and its immediate structural interactions may play a role in cellular folding providing a stable helix to anchor in the membrane, since helix I is presumably the first helix to fold and emerge from the translocon into the bilayer during co-translational folding of LacY. This is in line with results on the archaebacterial protein bacteriorhodopsin, where helix I of this 7 helical protein inserts first during cellular folding, is structured in the folding transition state, and is inherently stable as an individual helix *in vitro* [30; 32]. Insertion of the second, C domain of LacY does not appear to require the equivalent regions of the domain at the initial helix of the C domain to have enhanced stability. This is despite the fact

that that the C domain can be expressed and folded in the absence of the N domain [32], and that the two domains exhibit pseudo symmetry and are thought to arise from gene duplication [33].

Interestingly, the relative instability associated with the cytoplasmic end of helix VII, compared to the equivalent location on the N domain at the end of helix I, found here *in vitro* also correlates with the influence of native lipids on LacY folding and domain topology during cellular biogenesis. The natural membrane of LacY is dominated by phosphatidylethanolamine (PE) lipids. In *E. coli* strains lacking PE, the whole of the N domain of LacY is inverted in the membrane, which is enabled by helix VII of the C domain acting as a hinge and exiting the membrane; this in turn alters the overall fold of the C domain notably with the loss of packing interactions of helix VII [1; 34]. The relatively low hydrophobicity of helix VII, due to the presence of two negatively charged residues D237 and D240, could contribute to the unpacking of this helix and emergence into the periplasm.

Domain interface and accessibility

The stability of LacY can be increased with mutations at the domain interface that can stabilise a certain conformation, leading to further interactions between the domains and reducing the aqueous accessibility of this region. These stabilising mutations will also reduce access of denaturants such as urea to the domain interface and substrate binding pocket, leading to less denaturation than for the flexible WT protein.

The increased stability of the Tyr mutants stems primarily from mutation of W151 to Tyr; thus WT stability is observed for $W151_{Tyr}$ which retains the native W151. W151 forms part of the substrate binding site at the domain interface in LacY (Fig 1), forming interactions with the substrate via aromatic stacking between the indole of W151 and the sugar galactopyranosyl rings. Fluorescence quenching studies with $F261W_{Tyr}$ and $F261W_{Phe}$ show that the stable Tyr background mutants have lower aqueous accessibility at the domain interface than the less stable Phe mutants. Thus, increased stability correlates with reduced accessibility to the hydrophilic binding site, which is likely to result from reduced interdomain flexibility.

The newly introduced Tyr residue at position 151 in LacY mutant W151Y could stabilise the protein as a result of additional interactions that are absent in native LacY. Initial studies of potential hydrogen bonds involving W151Y across the domain interface suggest that there is a network of interactions or hydrogen bonds. This stabilising network of the new Tyr at position 151 and the native residues E269 andH322 contribute to the increased stability of W151Y, as removing these interactions by mutating E269 and H322 reduces the stabilising effect of W151Y. The effect is complicated however and does not arise from a single bond to E269, since mutating E269 has little effect on W151Y, but nearly eliminates the stabilising effect of W151Y when additional native Trps are mutated to Tyr. Both E269 and H322 are essential for LacY transport and function [35]. E269 is vital to both H^+ translocation and substrate recognition, and H322 for H^+ translocation. A hydrogen bond between W151 and E269 in the binding site has been proposed that could

be altered with Tyr at position 151 as opposed to Trp [36], although in this earlier study the stabilising C154G mutation was also present, which could affect the interactions at the domain interface. The C154G mutation stabilises the protein, locking it in an inward open conformation capable of binding substrate but not of transport [37; 38; 39]. E269Q in conjunction with C154G decreases the stabilising influence of C154G alone.

Conclusions

Measurements of thermodynamic stability are rare for multi-domain α helical proteins. Here we extend our previous measurement of the unfolding free energy of GalP to another member of the MFS, LacY. LacY can be reversibly unfolded enabling the free energy changes associated with recovery of native helical structure and ligand binding activity to be determined. The free energy for the two MFS proteins is very similar, in spite of the high flexibility of LacY. Mutations at the interface of the two domains of LacY increase protein stability by reducing accessibility of the interface to the aqueous surroundings. A single point mutation at the interface of the two domains is sufficient to render LacY resistant to urea denaturation. Single Trp residues provide useful measures of local intrinsic stability across the two domains and reveal an enhanced stability and resistance to urea denaturation at the cytoplasmic end of helix I, compared to the rest of the protein.

Methods

Materials

All reagents were purchased from Sigma-Aldrich or Fisher Scientific UK Ltd, except where specified. All primers were synthesised by Eurofins. All enzymes used and the 1 kb DNA ladder were purchased from New England Biolabs, with the exception of Pfu polymerase which was purchased either from Fermentas (ThermoFisher Scientific), or Promega. <99.5 % DDM was purchased from Generon. All reagents used were of the highest available grade.

PCR mutagenesis

The kanamycin resistance containing plasmid pST-Blue-1 was used as a vector for all the molecular biology in this paper, in Novagen *E. coli* NovaBlue Singles Competent Cells, or One Shot Top10 Chemically Competent *E. coli*. All mutants were made by PCR site directed mutagenesis. To make the single Trp mutants, five Trps were replaced with Phe leaving one native Trp behind. To create the Tyr background single Trp mutants, the first half of the gene (up to residue 762) was synthesised by Eurofins MWG Operon as all six native Trps are in this first half. The synthesised fragment was then subcloned into the second half

of LacY via an AgeI restriction site. The desired Trps were then individually mutated back in to this Tyr background Trp-less DNA. Trp-less LacY DNA was used as a template to create F243W, F261W and L383W with the desired Phe or Tyr background. WT LacY was used as a template to mutate W151 to Tyr, i.e. the five other native Trps were not mutated. The mutations E269Q and H322F were put into the relevant background i.e. W151Y or $W10_{Tyr}$. All the mutations were confirmed by sequencing (Eurofins MWG Operon), and subcloned into a modified pET-28a expression vector containing a C-terminal His10 tag, using XbaI/XhoI restriction sites on either end of the gene.

Protein expression and purification

LacY was expressed in One Shot BL21-AI Chemically Competent *E. coli*, using the kanamycin resistance containing plasmid pET-28a. The cultures were grown at 37 °C in LB media, and induced with 0.1 % arabinose and 1 mM IPTG at an OD_{600} of 0.6 - 0.8 AU. The cells were harvested by centrifugation at 5000 g when growth became stationary. All buffers during purification contained 50 mM sodium phosphate (pH 7.4), 10 % (v/v) glycerol, 10 mM β-mercaptoethanol and 1 mM DDM, with additional components indicated in brackets. As the critical micelle concentration of DDM is increased by urea, a DDM concentration of 1 mM was used throughout to ensure DDM micelles are present at the highest urea concentration of 8 M that was used (Fig S8). Following growth and induction, the cells were cracked by microfluidiser, and the membranes sedimented by centrifugation at 100,000 g at 4 °C for 30 minutes (Beckman Coulter Optima L-80 XP Ultracentrifuge, rotor 70Ti). The pellets were resuspended in 20 ml solubilisation buffer (200 mM NaCl, 20 mM imidazole, 10 mM β-mercaptoethanol, 40 mM DDM, EDTA free protease inhibitor cocktail tablet (Roche Applied Science)) at 4 °C for two hours. The solubilised membranes were spun at 100,000 g at 4 °C for 30 minutes, and the supernatant retained for purification. This was loaded at 1 $ml.min^{-1}$ onto a 1 ml HisTrap HP Ni^{2+} affinity column (GE Healthcare), previously equilibrated in ten column volumes of binding buffer (20 mM imidazole). Following loading, five column volumes of binding buffer was applied to the column to ensure all the protein was bound to the column, and to wash unbound contaminating protein. The column was then washed with fifty column volumes of wash buffer (75 mM imidazole). The protein was eluted directly into a spin concentrator (Amicon Ultra 50 kDa MWCO, Millipore) with ten column volumes of elution buffer (500 mM imidazole). The β-mercaptoethanol concentration was decreased to 2 mM for subsequent steps. Imidazole was then removed by desalting (5ml HiTrap Desalting Column, GE Healthcare), and gel filtration was used to separate LacY monomers from higher order aggregates.

Equilibrium unfolding and refolding

LacY was unfolded and refolded using the same method as previously described [10], with the following modifications; LacY was unfolded for 5 mins, at pH 7.4 and at 25 °C. Either the fluorescence band maximum or CD signal at 222 nm were used for further analysis, and fitted as described [10]. Briefly, the equilibrium

unfolding curve was used to obtain a free energy value, as the higher protein concentration in these experiments increased the signal to noise ratio. The unfolding curve was fitted to a two-state folding equation where the mean residue ellipticity $\theta = \theta_F - \theta_U(\exp(m([\text{denaturant}]-C_m)/RT)/(1+\exp(m([\text{denaturant}]-C_m)/RT)$. θ_F and θ_U are the CD values of the folded and unfolded states (or similarly for the fluorescence data), and C_m is the midpoint where there are equal amounts of folded and unfolded protein. The free energy of unfolding in the absence of denaturant is obtained from the fitted values, where $\Delta G_{u,}^{H_2O} = mC_m$. The non-linear regression was carried out using Grafit software (Erithacus) and the standard error of the best-fit curve calculated from the residuals.

CD spectroscopy

All CD spectra were measured in an Aviv Circular Dichroism Spectrophotometer, Model 410 (Biomedical Inc, Lakewood, NJ USA), with specially adapted sample detection to eliminate scattering artefacts, or at the Karlsruhe synchrotron (UV-CD12 beamline at ANKA, Karlsruhe Institute of Technology). A final protein concentration of 0.1 - 0.5 mg.ml^{-1} was used in quartz rectangular or circular Suprasil demountable cells of pathlengths 0.1 mm, 0.2 mm or 0.5 mm (Hellma Analytics). Each sample was scanned two to four times from 260 - 190 nm, at 1 nm intervals with an averaging time of 0.5 s. Samples containing urea were scanned from 260 - 200 nm due to the high absorbance of urea below 200 nm. The same cell containing buffer only was also measured for background subtraction during data analysis. All CD spectra were processed using CDTool [40], Dichroweb [41] and GraFit. First, the multiple scans were averaged and the buffer background was subtracted. These subtracted spectra were zeroed and smoothed, which set the baseline at zero between 253 - 260 nm. These processed spectra were then imported in to GraFit for further analysis. The data was converted from mdeg to Mean Residue Ellipticity (MRE). The MRE at 222 nm was used for further analysis, by converting it into a percentage of folded protein i.e. 100 % is fully folded protein and 0 % is the amount of secondary structure remaining in 8 M urea. These percentages were then plotted against the urea concentration for comparison between mutants and fitting if appropriate.

ITC measurements of refolded protein

At least 2.5 mg of LacY was unfolded in 8 M urea for 5 minutes, and refolded by a ten times rapid dilution into buffer at 25 °C for 10 minutes, a scale up of the refolding experiments already described. Following the rapid dilution refolding step, the protein was concentrated at 16 °C (Amicon Ultra 50kDa MWCO, Millipore, Megafuge 1.0R centrifuge, Heraeus Instruments) until the protein concentration reached 1 mg.ml^{-1} as determined by the absorbance at 280 nm. The protein was then dialysed in buffer to remove any residual urea, and the same buffer was used to make 800 µM NPG. The ITC experiment was done at 25 °C, with a spacing time of 180 s between injections. All samples were thoroughly degassed before titration. Typically there was a first run of 5 µl and 10 µl injections to a total of 300 µl, followed by a second run of fifteen 20 µl

injections to ensure saturation of the binding sites. A corresponding run of ligand injected into buffer was done to subtract the heat of dilution from the binding heats.

Due to the small amount of heat evolved, it is necessary to adjust the baseline and area of integration of the raw injections, using the adjust baseline tool in the Origin software supplied with the Microcal VP-ITC. This was done for both the protein-ligand and buffer-ligand titrations. A linear fit was applied to the dilution heats of ligand injected into buffer, and this linear fit subtracted from the protein injections. Due to the loss of sample at the tip of the needle during equilibration at the start of each run, the first injection is always wrong and therefore removed from the dataset. As start of the binding isotherm cannot be measured in a low affinity interaction such as this, the stoichiometry of the interaction must be defined in order to fit the data. One and two site binding models both failed to fit the data, so the LacY NPG binding isotherm has been fit with the best fit for the dataset. A sequential model (n=2) was fit to the binding isotherm.

Fluorescence spectroscopy

All fluorescence experiments were recorded with a Fluoromax-2 (ISA Instruments, S.A Inc), using a 4 mm pathlength Starna Quartz cuvette and at a protein concentration of 0.025 $mg.ml^{-1}$. An excitation wavelength of 295 nm was used, with the emission spectrum recorded in 0.25 nm increments from 315-400 nm, and 5 nm bandwidths for both excitation and emission. In all experiments, a scan under identical conditions without protein was also measured, and this background was subtracted from the protein scan. For samples containing urea, an individual scan at each denaturant concentration was required due to its emission peak at 330 nm. The raw fluorescence spectra were imported into GraFit5 (Erithacus), and the relevant background scans were subtracted from each protein scan. Each subtracted spectrum was fitted to an asymmetric peak function to ascertain the wavelength and intensity of the emission band maximum.

Acrylamide quenching

The degree of acrylamide quenching of intrinsic Trp fluorescence was measured as an indicator of solvent accessibility. Fluorescence intensity of each sample in 0 - 0.3 M acrylamide was measured, in 0.5 M steps. A sample containing only buffer was also measured for subtraction of the background fluorescence. The fluorescence intensity at the emission band maximum was used for further analysis. F_o/F_x was plotted against acrylamide concentration, the original fluorescence in absence of acrylamide being F_o, and the fluorescence at each acrylamide concentration being F_X. A linear fit was applied to F_o/F_x, which gave the Stern-Volmer constant, K_{SV}, in M^{-1}.

Acknowledgments

We are very grateful to Ron Kaback for providing LacY plasmids, advice on mutant LacY stability and function as well as comments on the manuscript. This work was funded by the BBSRC (studentship to NJH and research grants BB/F013183/1 and G008833/1 to PJB) and the European Research Council (Advanced Grant 294342 to PJB). PJB also thanks the Royal Society for a Wolfson Research Merit Award and the Leverhulme Trust for a Research Fellowship.

References

1. Vitrac, H., Bogdanov, M., Heacock, P. & Dowhan, W. (2011). Lipids and topological rules of membrane protein assembly: balance between long- and short-range lipid-protein interactions. *J Biol Chem*.
2. Curran, A. R., Templer, R. H. & Booth, P. J. (1999). Modulation of folding and assembly of the membrane protein bacteriorhodopsin by intermolecular forces within the lipid bilayer. *Biochemistry* **38**, 9328-36.
3. Allen, S. J., Curran, A. R., Templer, R. H., Meijberg, W. & Booth, P. J. (2004). Controlling the folding efficiency of an integral membrane protein. *J Mol Biol* **342**, 1293-304.
4. Miller, D., Charalambous, K., Rotem, D., Schuldiner, S., Curnow, P. & Booth, P. J. (2009). In vitro unfolding and refolding of the small multidrug transporter EmrE. *J Mol Biol* **393**, 815-32.
5. Seddon, A. M., Lorch, M., Ces, O., Templer, R. H., Macrae, F. & Booth, P. J. (2008). Phosphatidylglycerol lipids enhance folding of an alpha helical membrane protein. *J Mol Biol* **380**, 548-56.
6. Curnow, P. & Booth, P. J. (2007). Combined kinetic and thermodynamic analysis of alpha-helical membrane protein unfolding. *Proc Natl Acad Sci U S A* **104**, 18970-5.
7. Lau, F. W. & Bowie, J. U. (1997). A method for assessing the stability of a membrane protein. *Biochemistry* **36**, 5884-92.
8. Barrera, F. N., Renart, M. L., Poveda, J. A., de Kruijff, B., Killian, J. A. & Gonzalez-Ros, J. M. (2008). Protein self-assembly and lipid binding in the folding of the potassium channel KcsA. *Biochemistry* **47**, 2123-33.
9. Roman, E. A., Arguello, J. M. & Gonzalez Flecha, F. L. (2010). Reversible unfolding of a thermophilic membrane protein in phospholipid/detergent mixed micelles. *J Mol Biol* **397**, 550-9.
10. Findlay, H. E., Rutherford, N. G., Henderson, P. J. & Booth, P. J. (2010). Unfolding free energy of a two-domain transmembrane sugar transport protein. *Proc Natl Acad Sci U S A* **107**, 18451-6.
11. Huysmans, G. H., Baldwin, S. A., Brockwell, D. J. & Radford, S. E. (2010). The transition state for folding of an outer membrane protein. *Proc Natl Acad Sci U S A* **107**, 4099-104.
12. Boudker, O. & Verdon, G. (2010). Structural perspectives on secondary active transporters. *Trends Pharmacol Sci* **31**, 418-26.
13. Smirnova, I., Kasho, V. & Kaback, H. R. (2011). Lactose permease and the alternating access mechanism. *Biochemistry* **50**, 9684-93.
14. Madej, M. G., Soro, S. N. & Kaback, H. R. (2012). Apo-intermediate in the transport cycle of lactose permease (LacY). *Proc Natl Acad Sci U S A* **109**, E2970-8.
15. Huang, Y., Lemieux, M. J., Song, J., Auer, M. & Wang, D. N. (2003). Structure and mechanism of the glycerol-3-phosphate transporter from Escherichia coli. *Science* **301**, 616-20.
16. Guan, L., Mirza, O., Verner, G., Iwata, S. & Kaback, H. R. (2007). Structural determination of wild-type lactose permease. *Proc Natl Acad Sci U S A* **104**, 15294-8.
17. Yin, Y., He, X., Szewczyk, P., Nguyen, T. & Chang, G. (2006). Structure of the multidrug transporter EmrD from Escherichia coli. *Science* **312**, 741-4.
18. Dang, S., Sun, L., Huang, Y., Lu, F., Liu, Y., Gong, H., Wang, J. & Yan, N. (2010). Structure of a fucose transporter in an outward-open conformation. *Nature* **467**, 734-8.
19. Newstead, S., Drew, D., Cameron, A. D., Postis, V. L., Xia, X., Fowler, P. W., Ingram, J. C., Carpenter, E. P., Sansom, M. S., McPherson, M. J., Baldwin, S. A. & Iwata, S. (2011). Crystal structure of a

prokaryotic homologue of the mammalian oligopeptide-proton symporters, PepT1 and PepT2. *EMBO J* **30**, 417-26.
20. Solcan, N., Kwok, J., Fowler, P. W., Cameron, A. D., Drew, D., Iwata, S. & Newstead, S. (2012). Alternating access mechanism in the POT family of oligopeptide transporters. *EMBO J* **31**, 3411-21.
21. Sun, L., Zeng, X., Yan, C., Sun, X., Gong, X., Rao, Y. & Yan, N. (2012). Crystal structure of a bacterial homologue of glucose transporters GLUT1-4. *Nature* **490**, 361-6.
22. Quistgaard, E. M., Low, C., Moberg, P., Tresaugues, L. & Nordlund, P. (2013). Structural basis for substrate transport in the GLUT-homology family of monosaccharide transporters. *Nat Struct Mol Biol* **20**, 766-8.
23. le Coutre, J., Narasimhan, L. R., Patel, C. K. & Kaback, H. R. (1997). The lipid bilayer determines helical tilt angle and function in lactose permease of Escherichia coli. *Proc Natl Acad Sci U S A* **94**, 10167-71.
24. Abramson, J., Smirnova, I., Kasho, V., Verner, G., Kaback, H. R. & Iwata, S. (2003). Structure and mechanism of the lactose permease of Escherichia coli. *Science* **301**, 610-5.
25. Lau, F. W. & Bowie, J. U. (1997). A method for assessing the stability of a membrane protein. *Biochemistry* **36**, 5884-5892.
26. Curnow, P. & Booth, P. J. (2007). Combined kinetic and thermodynamic analysis of alpha-helical membrane protein unfolding. *Proc Natl Acad Sci U S A* **104**, 18970-18975.
27. Frillingos, S., Sahin-Toth, M., Wu, J. & Kaback, H. R. (1998). Cys-scanning mutagenesis: a novel approach to structure function relationships in polytopic membrane proteins. *Faseb J* **12**, 1281-99.
28. Weitzman, C., Consler, T. G. & Kaback, H. R. (1995). Fluorescence of native single-Trp mutants in the lactose permease from Escherichia coli: structural properties and evidence for a substrate-induced conformational change. *Protein Sci* **4**, 2310-8.
29. Menezes, M. E., Roepe, P. D. & Kaback, H. R. (1990). Design of a membrane transport protein for fluorescence spectroscopy. *Proc Natl Acad Sci U S A* **87**, 1638-42.
30. Curnow, P. & Booth, P. J. (2009). The transition state for integral membrane protein folding. *Proc Natl Acad Sci U S A* **106**, 773-8.
31. Vazquez-Ibar, J. L., Guan, L., Svrakic, M. & Kaback, H. R. (2003). Exploiting luminescence spectroscopy to elucidate the interaction between sugar and a tryptophan residue in the lactose permease of Escherichia coli. *Proc Natl Acad Sci U S A* **100**, 12706-11.
32. Curnow, P., Di Bartolo, N. D., Moreton, K. M., Ajoje, O. O., Saggese, N. P. & Booth, P. J. (2011). Stable folding core in the folding transition state of an alpha-helical integral membrane protein. *Proc Natl Acad Sci U S A* **108**, 14133-8.
33. Reddy, V. S., Shlykov, M. A., Castillo, R., Sun, E. I. & Saier, M. H., Jr. (2012). The major facilitator superfamily (MFS) revisited. *FEBS J* **279**, 2022-35.
34. Bogdanov, M., Xie, J., Heacock, P. & Dowhan, W. (2008). To flip or not to flip: lipid-protein charge interactions are a determinant of final membrane protein topology. *J Cell Biol* **182**, 925-35.
35. Guan, L. & Kaback, H. R. (2006). Lessons from lactose permease. *Annu Rev Biophys Biomol Struct* **35**, 67-91.
36. Vazquez-Ibar, J. L., Guan, L., Weinglass, A. B., Verner, G., Gordillo, R. & Kaback, H. R. (2004). Sugar recognition by the lactose permease of Escherichia coli. *J Biol Chem* **279**, 49214-21.
37. Smirnova, I. N. & Kaback, H. R. (2003). A mutation in the lactose permease of Escherichia coli that decreases conformational flexibility and increases protein stability. *Biochemistry* **42**, 3025-31.
38. Ermolova, N. V., Smirnova, I. N., Kasho, V. N. & Kaback, H. R. (2005). Interhelical packing modulates conformational flexibility in the lactose permease of Escherichia coli. *Biochemistry* **44**, 7669-77.
39. Nie, Y., Sabetfard, F. E. & Kaback, H. R. (2008). The Cys154-->Gly mutation in LacY causes constitutive opening of the hydrophilic periplasmic pathway. *J Mol Biol* **379**, 695-703.
40. Lees, J. G., Smith, B. R., Wien, F., Miles, A. J. & Wallace, B. A. (2004). CDtool-an integrated software package for circular dichroism spectroscopic data processing, analysis, and archiving. *Anal Biochem* **332**, 285-9.
41. Whitmore, L. & Wallace, B. A. (2004). DICHROWEB, an online server for protein secondary structure analyses from circular dichroism spectroscopic data. *Nucleic Acids Res* **32**, W668-73.

Figure Legends

Figure 1- Positions of Trp reporters in LacY

The location of each single Trp reporter is highlighted. The corresponding pairs of Trps on each domain have been coloured the same; W10 and W223 are orange, W33 and F243W are green, W171 and L383W are purple and F261W and W151 are red. W78 is coloured cyan and does not have a partner in the opposite domain. **A** LacY is shown perpendicular to the membrane, with the N domain on the right, the C domain on the left, and the cavity open towards the cytoplasm. **B** The view of LacY from the periplasm, with the C domain on the left. In A and B helices I and VII have been highlighted in blue. These figures were made in PyMOL (v 0.99, DeLano Scientific) using PDB file 2V8N. **C** Simplified cartoon of Trp positions in LacY. W10, W33, W151, W223, F243W, F261W have been highlighted with larger text.

Figure 2- Refolding of WT LacY reported by CD spectroscopy

A. Folded WT LacY was incubated in DDM (solid black line) and or 8 M urea (solid red line) for 5 min at room temperature. The latter was diluted into DDM for 10 mins, giving refolded LacY (dashed green line). Residual urea was removed from the refolded LacY sample by binding to Ni-NTA beads, followed by protein elution with 200 mM imidazole, which was removed by dialysis (solid blue line). Deconvolution of this spectrum estimated the α helical content as 83 % helix i.e. the native amount of helicity. **B** Unfolding (open circles) and refolding (black circles) of WT LacY measured by CD intensity at 222 nm. The amount of folded protein was determined from the degree of α helical structure as measured by the CD intensity at 222 nm, and the resulting values normalised between 0 % and 100 %. The latter represents the fully folded protein in DDM (with 85 % helix) and the former 0 % represents the urea-unfolded state that is partly structured (with approximately 55 % helix, see Fig 2A). The solid line represents a two state fit to the unfolding data. Unfolding was measured in a 0.2 mm pathlength cell at 0.15 – 0.24 mg.ml^{-1} LacY, with each data point being the result of twelve repeats giving a mean SE for the two state fit of ±9.64 %. Refolding was measured at 0.05mg.ml^{-1} LacY in a 0.5mm pathlength cell, and data points are the result of six repeats with a mean SE of ±10.9 %. The SE for data at 1M urea was ±4 %.

Figure 3– Unfolding of single Trp mutants $W33_{Phe}$, $W33_{Tyr}$, $F243W_{Phe}$ and $W223_{Phe}$

A CD spectra for Phe background mutants $F243W_{Phe}$ (left panel) and $W33_{Phe}$ (right panel) folded in DDM (black line) and unfolded in 8 M urea (red line). Spectra for the Tyr background mutant $W33_{Tyr}$ are also shown: in DDM (solid blue line) and 8 M urea (dashed red line). $F243W_{Phe}$ was measured at a concentration of 0.15 mg.ml^{-1}, $W33_{Phe}$ at 0.3 mg.ml^{-1} and $W33_{Tyr}$ at 0.13 mg.ml^{-1}. **B** Fluorescence-derived unfolding and refolding curves from the urea dependence of the intrinsic Trp fluorescence bands. Left panels show changes in the Trp fluorescence band maximum with urea, during unfolding (open circles) and refolding

(filled circles) for F243W$_{Phe}$ (top panels) and W223$_{Phe}$ (bottom panels). The urea dependence of the intrinsic Trp fluorescence band maximum for W33$_{Phe}$ (triangles) is shown for comparison with F243W$_{Phe}$. A positive wavelength shift indicates a red-shift of the band to longer wavelengths, and the solid lines show 2 state fits to the unfolding data. The wavelength band shifts are calculated by setting the wavelength of the fluorescence emission band maximum at 0 M urea to 0. Right panels show linear free energy relationships for ΔG_U with urea concentration. Error bars are the result of two repeat experiments for F243W$_{Phe}$, three repeats experiments for W223$_{Phe}$ and four repeat experiments for W33$_{Phe}$. Protein concentration was 0.025 mg.ml^{-1} for each mutant. Schematic diagrams of the mutant proteins are shown in each case, with the two domains shown in blue and the approximate position of the single Trp indicated by a green circle for the pair W33 and F243W, and an orange circle for W223.

Figure 4 - Stabilising mutations as domain interface

A Secondary structure change in 8 M urea of W151Y**.** W151Y at 0.12 mg.ml^{-1} was incubated in 8 M urea and measured by CD to assess any change in structure. Native W151Y is shown in black, and W151Y in 8 M urea in red. **B** Quenching the intrinsic Trp fluorescence of F261W$_{Phe}$ and F261W$_{Tyr}$**.** Acrylamide quenching of F261W was measured in a Tyr and Phe background. F261W lies on the C domain, at the domain interface opposite W151. F261W$_{Phe}$ is shown in open circles and F261W$_{Tyr}$ in black circles. The gradient of the linear fit gives the K_{sv}, 1.67 ± 0.11 M^{-1} for F261W$_{Phe}$ and 0.52 ± 0.06 M^{-1} for F261W$_{Tyr}$. Errors are taken from the standard error of the linear fit, and error bars are the result of three repeats. Schematic diagrams of the mutant proteins are shown in each case, with the two domains shown in blue. The approximate positions of the Trps and the W151 Tyr mutation are labelled in green and red respectively, and the single Trp F261W indicated by a red circle.

Figure 5 - Domain interface mutations

A The domain interface mutations: C154G, W151Y, F261W, T265V, E269Q and H322F. This figure was made in PyMOL (v 0.99, DeLano Scientific) using PDB file 2V8N. The newly introduced residues are shown using the mutagenesis tool in PyMOL. **B** CD spectra for W10$_{Tyr}$/E269Q, whereall Trps are mutated to Tyr except W10. The folded state is shown by the black line, and unfolded in 8 M urea by the red line. In the accompanying schematic, the location of mutation E269Q is shown by a red star, and the locations of the native Trp W10 and the Tyr mutations have been labelled in green and purple respectively. **C** Schematic of locations of domain interface mutations, with the Trps labelled in green, and the domain mutations labelled in purple. **D** Mutation of potential hydrogen bonding partners of W151, H322F and E269Q, have limited effect on stability. CD spectra of W151Y/E269Q folded (solid black line) and unfolded in 8 M urea (solid red line), compared with W151Y/H322F folded (blue short dashes), and unfolded in 8 M urea (green long dashes). There is a small decrease in the amplitude of the peak at 222nm, but neither mutation

significantly destabilises W151Y. Note that in **A-C** these the N domain on the left and the C domain on the right.

Table 1

The ΔG_U^{H2O} values for WT and the Phe background single Trp mutants, derived from fluorescence and CD denaturation curves

ΔG_U^{H2O} values are determined from the red-shift observed in the Trp fluorescence band upon unfolding in urea, both by a two state fit to the denaturation curve as well as from linear extrapolation of ΔG_U at different urea concentrations. Values determined from CD denaturation curves are shown for comparison for WT LacY, as well as those mutants with sufficient high expression to obtain the larger amounts of protein and higher concentrations necessary for CD denaturation curves. There is good agreement between the fluorescence and CD-derived values. Errors are from the standard error of the fit.

Table 2

Single Trp mutant pairs which exhibit contrasting behaviour with respect to the local structurela environment of helices I and VII, as well as the domain interface, together with key findings. The single Trps which are in a hydrophobic environment in the folded structure are highlighted in grey.

Tables

Table 1

Mutant	*From two state fit*	*From linear extrapolation*
	ΔG_U^{H2O} (kcal.mol^{-1})	ΔG_U^{H2O} (kcal.mol^{-1})
Fluorescence		
$W10_{Phe}$	2.0 ± 0.4	2.1 ± 0.1
$W78_{Phe}$	2.2 ± 0.5	2.0 ± 0.2
$W151_{Phe}$	2.1 ± 0.4	2.2 ± 0.1
$W171_{Phe}$	3.3 ± 0.8	3.3 ± 0.3
$W223_{Phe}$	2.2 ± 0.4	2.2 ± 0.2
$F243W_{Phe}$	2.1 ± 0.2	2.2 ± 0.1
$L383W_{Phe}$	2.0 ± 0.2	1.9 ± 0.1
$F261W_{Phe}$	2.3 ± 0.5	2.2 ± 0.2
CD		
WT	2.7 ± 0.6	2.6 ± 0.4
$W33_{Phe}$	2.7 ± 1.8	2.3 ± 0.6
$W223_{Phe}$	2.3 ± 1.1	2.2 ± 0.5

Table 2

Mutant	Helix number and domain	Environment	Key finding
$W10_{Tyr}$ $W223_{Tyr}$	I, N domain VII, C domain	Cytoplasmic end of helix	Local unfolding at cytoplasmic end of helix VII
$W33_{Phe}$ $F243W_{Phe}$	I, N domain VII, C domain	Periplasmic end at helix interface	Enhanced stability of helix I compared to helix VII & WT
$W151_{Tyr}$ $F261W_{Tyr}$	V, N domain VIII, C domain	Domain interface	Increased stability reflects reduced accessibility to domain interface

Figure 1

Click here to download high resolution image

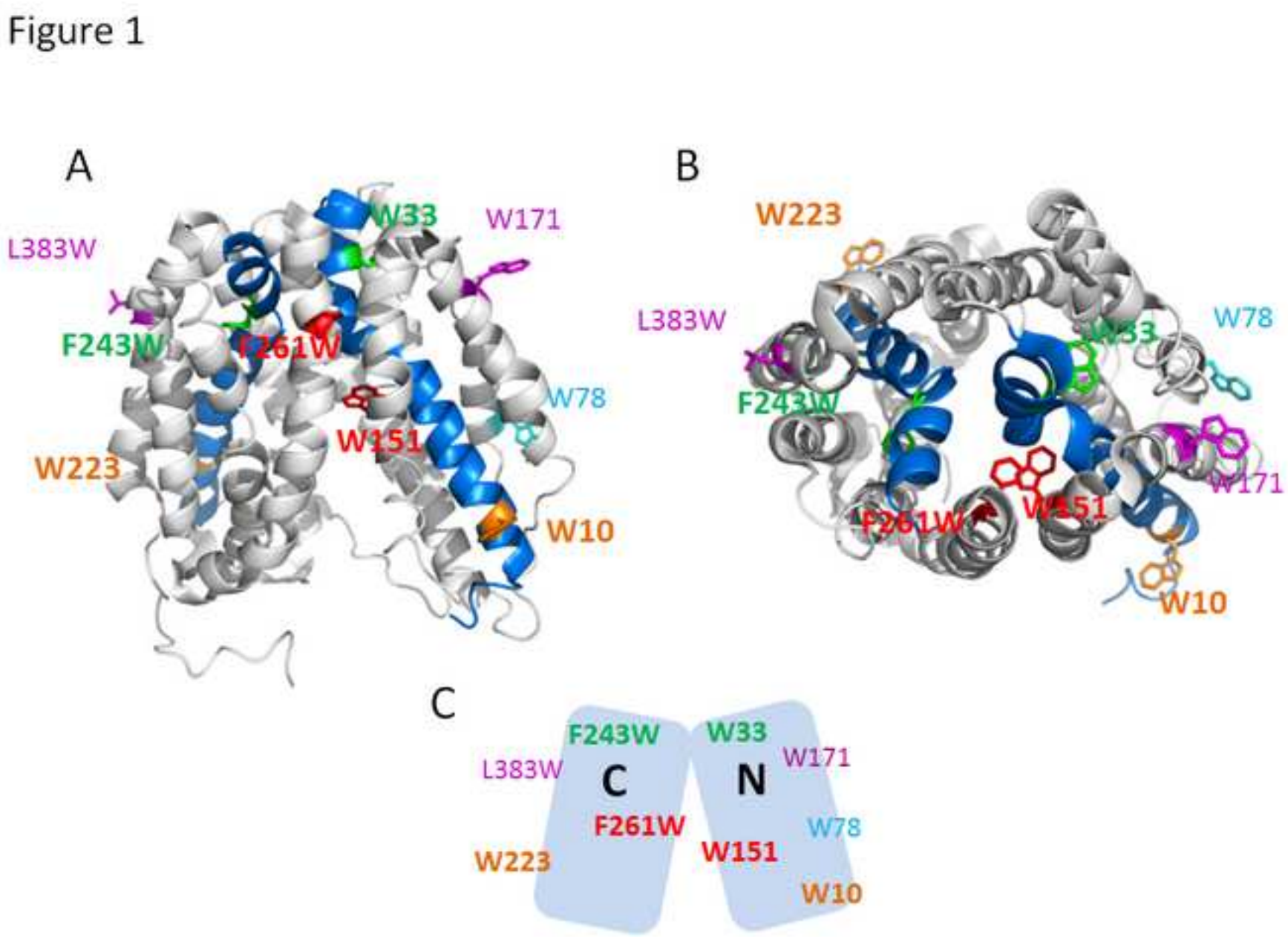

Figure 2

Click here to download high resolution image

Figure 2

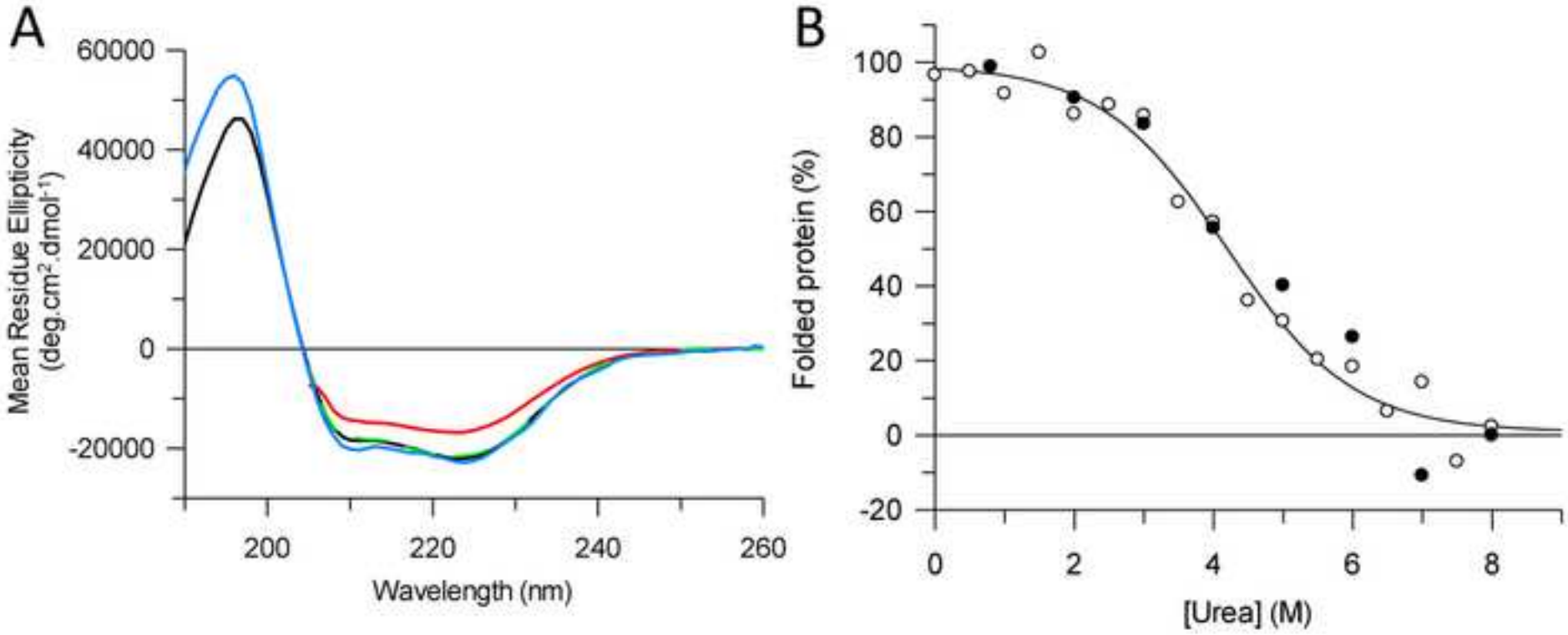

Figure 3

Click here to download high resolution image

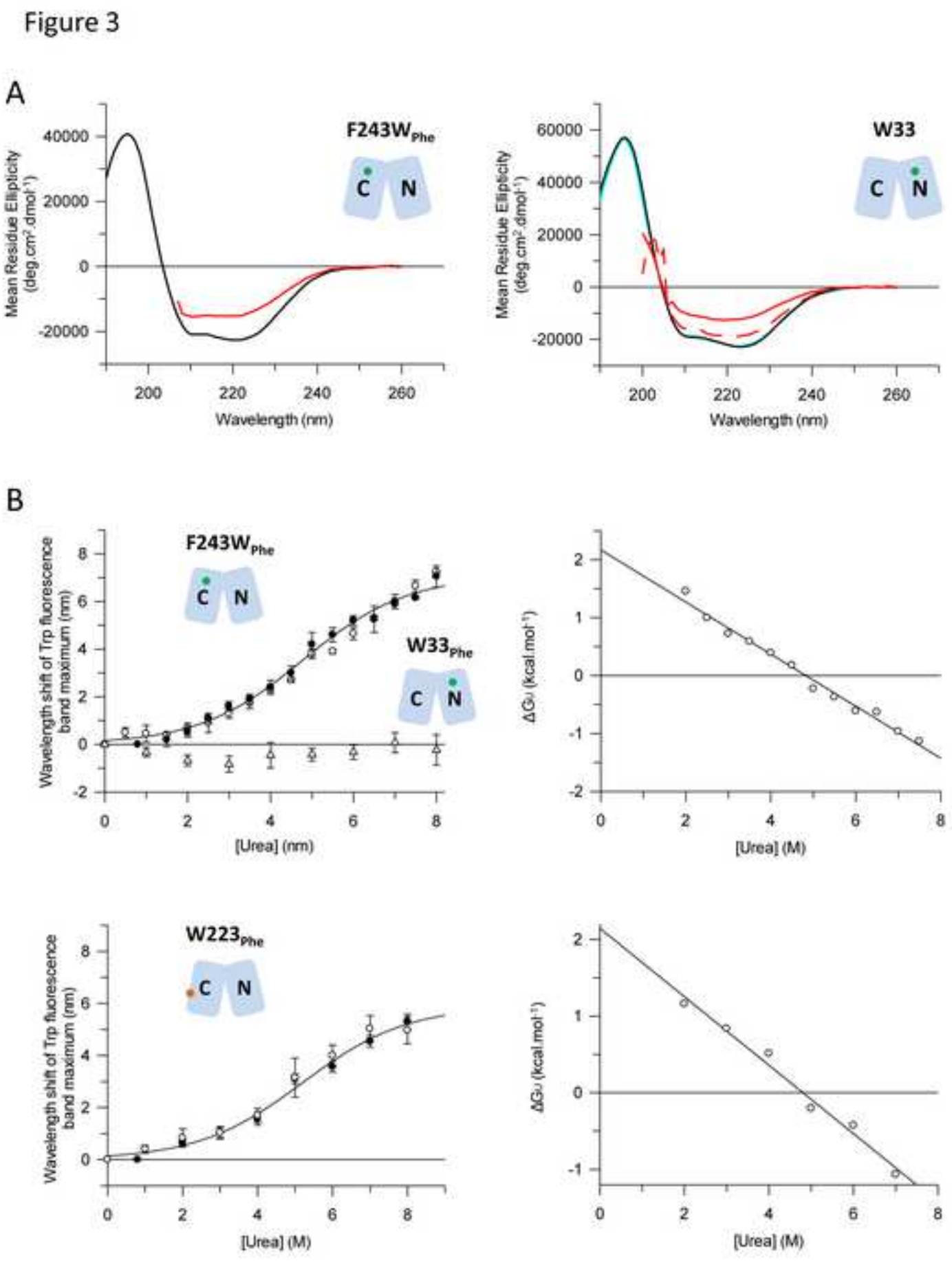

Figure 4

Click here to download high resolution image

Figure 4

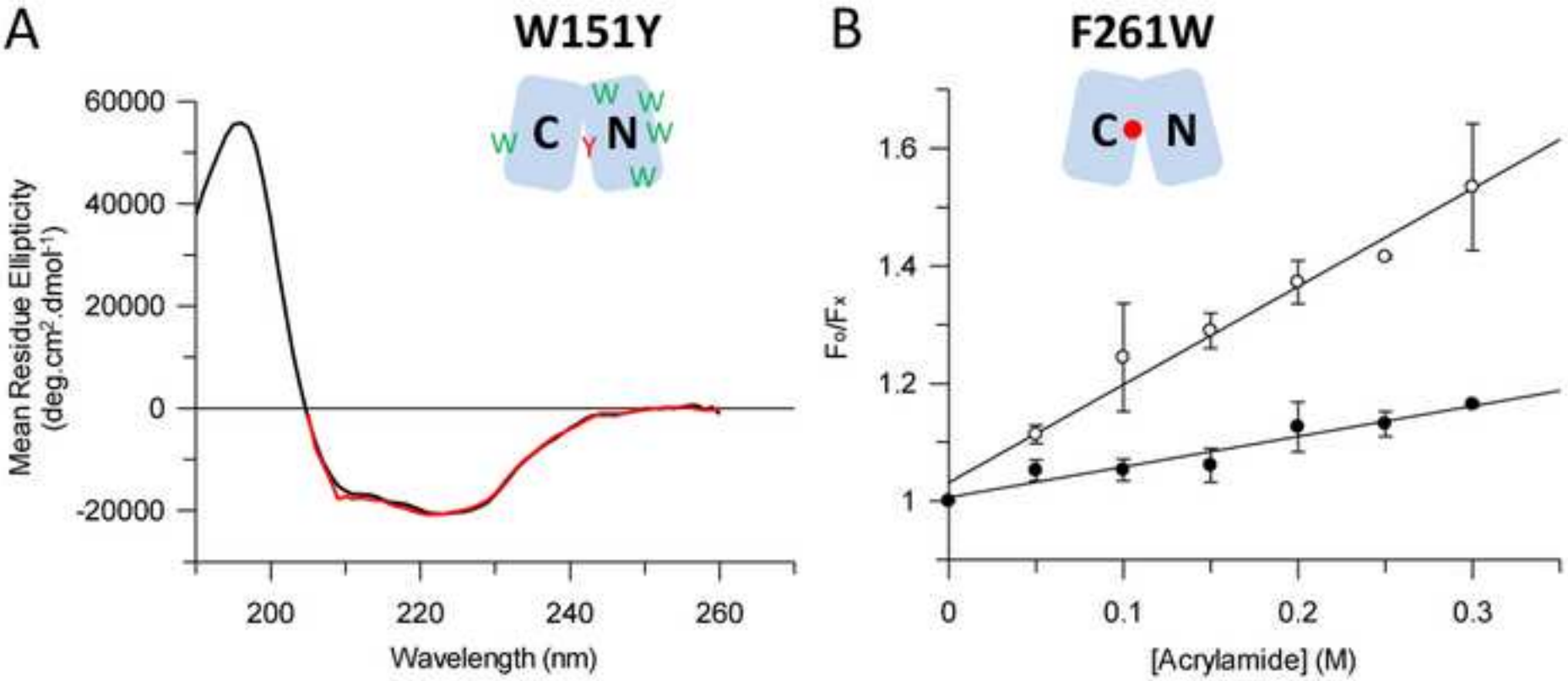

Figure 5
Click here to download high resolution image

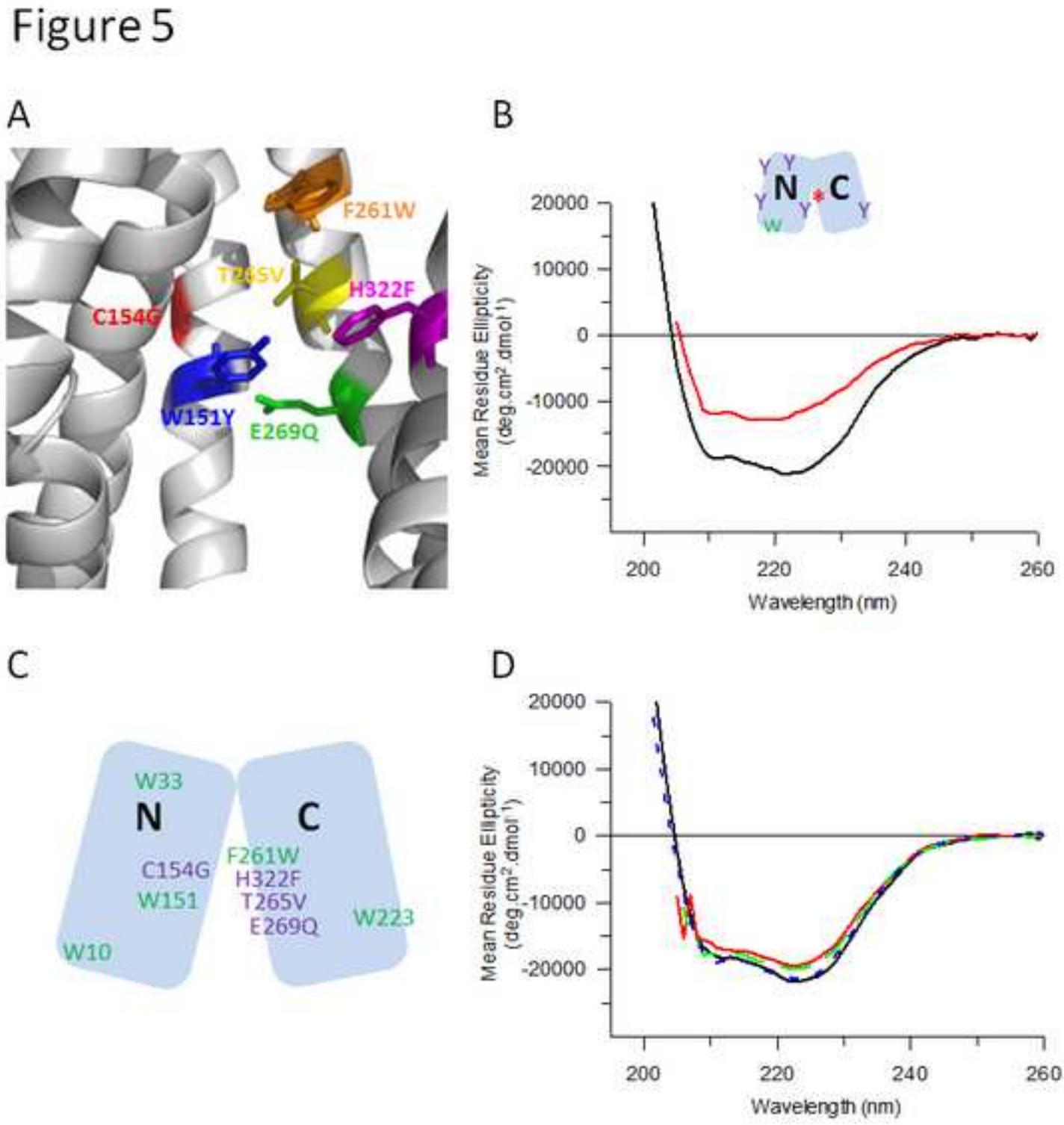

Supplementary marked

Click here to download Supplementary Material (To be Published): Harris et al SI revised marked.docx

Supplementary unmarked

Click here to download Supplementary Material (To be Published): Harris et al SI revised unmarked.docx